Hybridization dynamics and extensive introgression in the *Daphnia longispina* species complex: new insights from a high-quality *Daphnia galeata* reference genome

Jana Nickel[1], Tilman Schell[2], Tania Holtzem[3], Anne Thielsch[4], Stuart R. Dennis[5], Birgit C. Schlick-Steiner[3], Florian M. Steiner[3], Markus Möst[3], Markus Pfenninger[2,6,7], Klaus Schwenk[4], Mathilde Cordellier[1*]

[1] Institute of Zoology, Universität Hamburg, Germany

[2] LOEWE Centre for Translational Biodiversity Genomics (LOEWE-TBG), Frankfurt am Main, Germany

[3] Department of Ecology, University of Innsbruck, Innsbruck, Austria

[4] Molecular Ecology, Institute for Environmental Sciences, University Koblenz-Landau, Landau in der Pfalz, Germany

[5] Dept of Aquatic Ecology, EAWAG Dübendorf, Switzerland

[6] Molecular Ecology, Senckenberg Biodiversity and Climate Research Centre, Frankfurt, Germany

[7] IoME, Gutenberg University, Mainz, Germany

*corresponding author: Mathilde Cordellier, Department of Biology, Institute of Zoology, University of Hamburg, Hamburg, Germany, mathilde.cordellier@uni-hamburg.de

Abstract

Hybridization and introgression are recognized as an important source of variation that influence adaptive processes; both phenomena are frequent in the genus *Daphnia,* a keystone zooplankton taxon in freshwater ecosystems that comprises several species complexes. To investigate genome-wide consequences of introgression between species, we provide here the first high-quality genome assembly for a member of the *Daphnia longispina* species complex, *Daphnia galeata*. We further re-sequenced 49 whole genomes of three species of the complex and their interspecific hybrids both from genotypes sampled in the water column and from single resting eggs extracted from sediment cores. Populations from habitats with diverse ecological conditions offered an opportunity to study the dynamics of hybridization linked to ecological changes and revealed a high prevalence of hybrids. Using phylogenetic and population genomic approaches, we provide first insights into the intra- and interspecific genome-wide variability in this species complex and identify regions of high divergence. Finally, we assess the length of ancestry tracts in hybrids to characterize introgression patterns across the genome. Our analyses uncover a complex history of hybridization and introgression reflecting multiple generations of hybridization and backcrossing in the *Daphnia longispina* species complex. Overall, this study and the new resources presented here pave the way for a better understanding of ancient and contemporary gene flow in the species complex and facilitate future studies on resting egg banks accumulating in lake sediment.

Keywords

introgression, hybridization, resting eggs, species complex, whole-genome amplification, genome assembly

Introduction

Gene flow between species can be pervasive and can affect substantial parts of the genome. Hybridization and introgression are recognized as an important source of variation that can influence adaptive processes in plants, animals, yeast, and fungi (reviewed in Abbott*, et al.* 2013; Arnold and Martin 2009). The amount of realized gene flow varies among taxa and along the genome; it is governed by intrinsic genomic features such as recombination rate, structural variation and intrinsic incompatibilities, as well as the species' biology and ecology including ecological and sexual selection, migration, and mode of reproduction.

How can species in diversifying clades frequently hybridize and show introgression but nevertheless maintain species boundaries? A growing body of literature provides examples for a high variety of systems where speciation occurs in the face of gene flow (e.g. Fraïsse*, et al.* 2014; Martin*, et al.* 2019; Meier*, et al.* 2017). However, it is important to recognize that these systems are distributed along a wide spectrum. On one side of this spectrum, hybridization occurs but is not followed by introgression for several reasons such as reduced hybrid fertility or strong selection against hybrid phenotypes, leading to rapid hybrid breakdown. Barth*, et al.* (2020) found that species boundaries in tropical eels are stable despite millions of years of hybridization, and also observed very few admixed individuals beyond F1 and first-generation backcrosses. The hybrid breakdown observed in this system reduces the likelihood of introgression via backcrossing. On the other side of the spectrum, hybridization is followed by introgression, and ongoing exchange of genetic information between species (e.g. Butlin*, et al.* 2014; Doellman*, et al.* 2018; Kaiser*, et al.* 2021; Martin*, et al.* 2013). Several empirical studies (Canestrelli*, et al.* 2017; Schreiber and Pfenninger) as well as theoretical models (Flaxman*, et al.* 2014; Rafajlović*, et al.* 2016; Yeaman and Whitlock 2011) suggest the possibility of intermediate constant equilibrium states, meaning that certain parts of the genome remain diverged ('islands' or 'continents of divergence'), while others are freely exchanged among closely related species without ever reaching complete genomic isolation.

Recurrent hybridization and introgression are frequent in the genus *Daphnia* (Crustacea, Cladocera) Members of the genus have served as ecological model organisms for over a century (e.g. Miner*, et al.*

2012), and the first crustacean genome to be sequenced was that of a member of the *Daphnia pulex* species complex (Colbourne*, et al.* 2011). Since then, the genomes of 45 crustaceans have been sequenced with a focus on species of economic or medical interest (NCBI, last accessed January 2021). Despite their key role in marine and freshwater food webs around the globe, genomic resources for zooplanktonic species are still scarce. In many aquatic food webs, zooplanktonic crustaceans link primary production by phytoplankton and secondary consumers, such as planktivorous fish and larger invertebrate species (Lampert and Sommer 2007). (e.g. Gannon and Stemberger 1978; Gliwicz 1990)

Daphnia are highly phenotypically plastic and a textbook example for inducible defense mechanisms (Tollrian and Harvell 1999), as they respond to variation in predation risk through spectacular changes in morphology. Further, *Daphnia* are cyclical parthenogens and hence able to alternate between asexual and sexual reproduction. They reproduce asexually through longer periods of time, and the product of sexual reproduction events (usually seasonal) are resting eggs able to withstand adverse conditions for decades and even centuries (Frisch*, et al.* 2014). Resting eggs extracted from sediment cores can be hatched, and ancient genotypes brought to life (reviewed in Orsini*, et al.* 2013). Moreover, the DNA preserved in those resting eggs can be directly analyzed with various molecular methods (e.g. Cousyn*, et al.* 2001; Dziuba*, et al.* 2020; Lack*, et al.* 2018). Thus, cyclical parthenogenesis, biological archives in lake sediments and high levels of phenotypic plasticity make *Daphnia* a particularly interesting model for evolutionary studies.

The genus *Daphnia* is composed of two subgenera, *Ctenodaphnia* and *Daphnia*, and two groups are delimited within the subgenus *Daphnia*: the *D. pulex* group *sensu lato* and the *D. longispina* group *sensu lato* (see Adamowicz*, et al.* 2009). The latter is sometimes also referred to as subgenus *Hyalodaphnia* and includes the *Daphnia longispina* species complex (DLSC) (Petrusek*, et al.* 2008a). The two *Daphnia* groups are highly differentiated and share their most recent common ancestor around 30 Mya (MRCA *D. longispina* – *D. pulex* group, MRCA *D. longispina* – *D. pulex* group, Cornetti*, et al.* 2019). Members of the genus *Daphnia* show little variation in chromosome number, with most species having 10 pairs of chromosomes, except for the *D. pulex* group with n=12 (Beaton and Hebert 1994; Trentini 1980). All sequenced and

92 assembled *Daphnia* genomes so far belong either to the *D. pulex* group or the subgenus *Ctenodaphnia*,
93 however no high-quality reference genome of the third major group, the *D. longispina* group
94 (*Hyalodaphnia*) is published.

95 The prevalence of hybridization in the genus *Daphnia* across taxa and ecosystems and its impact on their
96 evolutionary history has intrigued researchers for decades (e.g. Schwenk 1993; Vergilino, *et al.* 2011; Wolf
97 1987). In contrast to many other well-studied hybrid systems (Barton and Hewitt 1985) with clear defined
98 hybrid zones where species' ranges overlap, the distribution of *Daphnia* species and their hybrids is more
99 of a fragmented nature: they occupy lake and pond ecosystems that vary in their ecological characteristics
100 and hence constitute a mosaic across the landscape. Ecologically differentiated taxa and their hybrids are
101 thus distributed across habitat patches (Harrison 1986). Within these patches, the possibility to interrogate
102 biological archives also revealed fluctuations in *Daphnia* community composition over time (e.g. Alric, *et*
103 *al.* 2016; Brede, *et al.* 2009), associated with hybridization events among species in some cases. Variation
104 in hybridization events across time and among habitats has often been observed in correlation with
105 ecological changes, such as eutrophication or global change (Brede, *et al.* 2009; Cordellier, *et al.* 2021;
106 Dziuba, *et al.* 2020; Keller, *et al.* 2008; Rellstab, *et al.* 2011; Spaak, *et al.* 2012).

107 Members of the *Daphnia longispina* species complex inhabit many large ponds and lakes in central and
108 northern Europe, and three of them have been particularly well studied: *Daphnia galeata*, *Daphnia*
109 *longispina* and *Daphnia cucullata* (Petrusek, *et al.* 2008a). These species can coexist, but earlier studies
110 suggest gene flow among them is limited (Spaak 2004). Despite their obviously ancient divergence
111 (Schwenk, *et al.* 2000), DLSC species are still able to form interspecific hybrids, although not all
112 combinations are equally likely to lead to viable and fertile individuals (Schwenk, *et al.* 2001). A mechanism
113 preventing gene flow among species might be their different ecological preferences, e.g., regarding trophic
114 level (Spaak, *et al.* 2012), food quality (Seidendorf, *et al.* 2007), and predation pressure (Spaak and Hoekstra
115 1997);(Petrusek, *et al.* 2008b).

Up to now, genetic markers available to study hybridization in the DLSC are limited to allozymes (Wolf and Mort 1986), a few mitochondrial regions (Schwenk 1993), a dozen microsatellite markers (Brede, *et al.* 2006; Thielsch, *et al.* 2012) and a few further nuclear loci (Billiones, *et al.* 2004; Rusek, *et al.* 2015; Skage, *et al.* 2007). Seminal studies such as Brede, *et al.* (2009) and Limburg and Weider (2002) first made use of microsatellite markers to analyze environmentally driven shifts in allelic frequencies, species and hybrid composition of the DLSC communities in Lake Constance and Belauer See over time, respectively. Further, a number of studies addressed the spatial distribution of DLSC species/taxa with these markers (e.g. Griebel, *et al.* 2016; Ma, *et al.* 2019; Thielsch, *et al.* 2017). These low-resolution markers allowed to identify hybrid individuals and brought evidence for introgression but could not provide the resolution necessary to either assess how pervasive introgression is or how it varies across the genome. Further, it is not clear whether introgression occurs among all three species to the same extent. Given the ubiquitous hybridization among the DLSC taxa, the question also arises why they are still well distinguishable species. Whether the DLSC represents a case of incipient speciation, introgression after secondary contact, speciation reversal, or has reached an intermediate constant equilibrium state, among other possibilities, can only be answered with genome-wide analyses empowered by a high-quality genome assembly.

Here, we present a high-quality assembly for *Daphnia galeata*, thus filling an important gap for *Daphnia* whole-genome studies. Furthermore, to facilitate genome-wide assessments of divergence across species and of introgression between species, we conducted genome-wide resequencing studies in the DLSC. We analyzed whole-genome sequences of parental species and their interspecific hybrids, both from genotypes obtained in the wild and maintained in laboratories, and from single resting eggs extracted from sediment cores. We provide first insights into the intra- and interspecific genome-wide variability in this species complex and identify regions of high divergence. We reconstructed the phylogenetic relationships in the species complex using whole mitochondrial genomes. Finally, we assess the length of ancestry tracts in different classes of hybrids to characterize introgression patterns. Our study paves the way for long-awaited analyses on the dynamics of introgression in this complex and exploitation of the unique opportunity this group has to offer: a window of more than one hundred years of evolution in action.

Results

Genome assembly

The raw assembly was obtained by combining PacBio long reads (1,679,290, 11.52 Gb) and Illumina short reads (70,310,338, 9.79 Gb after trimming) and using the hybrid assembler RA (https://github.com/lbcb-sci/ra). It originally comprised 1,415 contig sequences covering a total length of 153.6 Megabases (Mb), with an N50 value of 172 kilobases (kb) and a slightly elevated GC content (40.02% Supplementary Methods Table 3) compared with the values expected for a *Daphnia* species (see Table 1). According to an analysis based on coverage and GC content of the contig sequences conducted with blobtools (Laetsch and Blaxter 2017), a portion of the assembly consisted of non-*Daphnia* contigs, which could then be removed (267 contigs, equaling 22.97 Mb). Consequently, GC content decreased to 38.75%, nearing the values obtained for other *Daphnia* assemblies (see Table 1 for an overview). The application of this filter as well as the exclusion of the mitochondrial genome led to a decrease in the number of sequences and the total length of the assembly. Iterative scaffolding led to a decrease in the total number of sequences. This together with a substantial increase in N50 resulted in a highly contiguous assembly, with a total length of 133,304,63 basepairs (bp), an N50 of 756.7 kb and only 346 sequences, i.e., on average 30 sequences per chromosome. Contiguity statistics for the different assembling steps are given in Supplementary Methods Table 3.

Mapping the filtered Illumina reads with bwa mem (Li 2013) and PacBio reads with Minimap 2.17 (Li 2018), resulted in a mapping rate of respectively 94.1% and 85.5%. The coverage distribution can be seen in Figure S1B.

According to blobtools results, no contamination could be identified in the final assembly (Figure S1A). Remaining scaffolds (12, amounting to a total length 1.79Mb) with taxonomic assignment other than Arthropoda were kept because coverage and GC are similar to *D. galeata* scaffolds and taxonomic assignment alone might be false positive. Further, the completeness assessment through BUSCO (Simão*, et al.* 2015, Arthropoda set, odb9) indicated 95.7% of complete single copy core orthologs and a very low duplication rate (C: 95.7% [S: 94.7%, D: 1.0%], F: 0.8%, M: 3.5%, n: 1066). The genome size was estimated

based on mapped nucleotides and mode of the coverage distribution by backmap 0.3 (https://github.com/schellt/backmap), resulting in 156.86Mb and 178.03Mb for Illumina (52x) and PacBio (26x) respectively, and by k-mer based approach using GenomeScope resulting in a size of 150.6Mb.

When compared to other published full genomes for *Daphnia* species, the *D. galeata* final assembly is shorter than both *D. pulex* assemblies (Colbourne*, et al.* 2011; Ye*, et al.* 2017), and roughly the same size as *D. magna* (Lee*, et al.* 2019), which also has 10 chromosomes (Table 1). The GC content is lower, which can be attributed to the strict filtering for contamination applied pre- and post-assembly, a procedure not applied in the other *Daphnia* assemblies, to our knowledge. Even though Lee *et al.* (2019) and Ye *et al.* (2017) treated the animals with antibotics before sequencing this suggests that these genome assemblies contain more contigs of bacterial origin than the *D. galeata* assembly. Thanks to the use of long-read data, iterative scaffolding and gap filling, the number and length of assembly gaps (Ns) is substantially lower and contiguity is high (but see Table 3 in Supplementary Methods).

Genome annotation

After applying RepeatMasker (Smit*, et al.* 2013-2015) with the custom repeat library described in the methods section, 21.9% of the assembly was masked. The distribution of masked fraction per repeat element can be found in Supplementary Methods Table 5.

The final annotation with MAKER (Holt and Yandell 2011) predicts 15,845 genes with a median length of 2,097 base pairs. There is an average of 1.06 mRNAs per gene and 7 exons/mRNA (Table 1). The total number of predicted mRNA substantially differs from the number of transcripts previously published for this species (32,903, Huylmans*, et al.* 2016). This is not surprising, as this transcriptome assembly did not make use of protein evidence we included here, and might contain isoforms. Further, it was based on a pool of mRNA from different clonal lines, and the assembly process might have been impeded by allelic diversity. As further quality criterion, the Annotation Editing Distance (AED) was compared across the three MAKER rounds and is visualized in Supplementary Methods Figure 4. AED improved mostly between rounds 1 and 2 of the annotation but only marginally with a further round.

Table 1: Assembly metrics and annotation statistics for the present assembly and two previously published *Daphnia* assemblies. Contiguity statistics of the annotation were calculated excluding tRNAscan results. BUSCO 3.0.2 was executed in protein mode for the different MAKER rounds. Conserved Domain Arrangements (CDAs) were searched with Pfam scan 1.6 and DOGMA 3.4. Results for BUSCO and DOGMA completeness statistics are given in percent.

Species	*D. galeata*	*D. pulex* (Ye *et al*)	*D. magna* (Lee *et al*)
Strain	M5	PA42	SK
Assembly metrics			
# scaffolds	346	493	4,192
Largest scaffold (bp)	2,950,711	7,584,612	16,359,456
Total length (bp)	133,304,630	189,550,516	122,937,721
N50 (bp)	756,671	1,160,003	10,124,675
L50 (bp)	48	36	5
GC (%)	38.75	40.39	40.54
# N's	120,845	4,006,006	82,97,703
# N's per 100 kbp	90.65	2113.42	6749.52
Annotation			
Number			
Gene	15,845	18,440	15,721
mRNA	16,774	18,440	15,721
Exon	117,364	128,688	95,203
CDS	119,402	118,916	94,047
Mean			
mRNAs/gene	1.06	1	1
Exons/mRNA	7.00	6.98	6.06
CDSs/mRNA	7.12	6.45	5.98
Median length (bp)			
Gene	2,097	1,919.5	1,586
mRNA	2,142	1,919.5	1,521
Exon	167	162	160
Intron	74		
CDS	152	144	159
Total space (bp)			
Gene	51,689,473	53,936,938	37,505,261
mRNA	51,689,329	53,936,938	36,178,687
Exon	29,314,592	30,208,483	22,336,755
CDS	25,132,876	23,586,918	21,881,778
Single			
Exon mRNA	663	144	1,775
CDS mRNA	710	0	0
BUSCO N=1066			
C	94.3	94.1	97.0
S	91.7	82.6	95.3

D	2.6	11.5	1.7
F	0.7	3.5	1.7
M	5.0	2.4	1.3
DOGMA N=4222	93.63	91.43	93.91

A high percentage of protein sequences could be annotated: 15,898 (94.78%) with InterProScan (Jones, *et al.* 2014) and 15,960 (95.15%) with blast against Swiss-Prot. With this combination of searches, a hit within InterProScan and blast was found for 16,675 protein sequences (99.41%). GeneOntology annotation was possible for 9555 sequences (56.96%). A detailed overview of the functional annotated sequences per database or search algorithm is shown in Supplementary Methods Table 7.

Genotyping

Short-read sequence data were generated for 72 individuals: 17 unamplified DNA samples from isofemale clonal lines and 55 whole genome amplification (WGA) samples (conducted on single resting eggs) that passed PCR contamination checks. After screening for contamination and removing datasets with only very few reads mapping to the *D. galeata* reference, 49 single genotypes remained: 32 from resting eggs and 17 from clonally propagated lines, established from individuals sampled in the water column or hatched from resting eggs (Figure 1A, Table S2). Data gained from clonal lines with a species attribution were used as "parental species" data: five samples for *D. galeata*, four for *D. longispina*, and three for *D. cucullata*. The parental clones are part of two larger clone panels representing the parental species and their diversity in several European lakes. Their identity was established prior to this study either based on mitochondrial and microsatellite markers (M5, LC3_6, J2, Herrmann, *et al.* 2017) or morphological examination, mitochondrial markers and factorial correspondence analyses based on microsatellite markers (Alric, *et al.* 2016; Möst 2013), including hybrids and historical resting eggs, which separates parental species and hybrids (e.g. Alric, *et al.* 2016; Dlouha, *et al.* 2010; Rellstab, *et al.* 2011; Yin, *et al.* 2014). In addition, data were available for four resting eggs from Arendsee (AR), 12 resting eggs from Dobersdorfer See (DOB), five clonal lines and eight resting eggs from Eichbaumsee (EIC), and eight resting eggs from Selenter See (SE) (Table S2). While the analysis of eggs from older sediment layers was attempted, biological material

was either limited, of poor quality, or contaminated. Our isotope dating for DOB was unconclusive: either slides of the cored location or a high sedimentation rate meant the top 30 cm of the core didn't show the usual isotope peaks, thus preventing precise dating. EIC samples were recent since they were collected from surface bank sand. For SE, the oldest eggs analyzed here originated from the 2-3cm layer of the core, which corresponds to max. ~17 years (pers. comm Thorbjørn Andersen). For AR the oldest eggs for which results were obtained were isolated from the 4-5cm layer, corresponding to ~2005 (pers. comm. Miklos Balínt).

An average of 89.9% (range: 31.7-98.6%) reads aligned to the reference genome with a mean coverage of 10.26x (range: 0.34-52.30x) (Table S3). The final SNP data set for subsequent analyses after quality-filtering included 3,240,339 SNPs across the 49 samples. To rule out possible reference bias we compared mapping rates of reads with the reference allele and to the alternative allele at heterozygous sites. We found no preferential mapping of the reference allele, as all species categories and the hybrids had a median distribution close to 0.5 (Figure S2).

Principal Component Analysis

In a PCA including all genotypes and conducted with SNPRelate v1.20.1 (Zheng*, et al.* 2012), the parental species genotypes grouped in three very distinct clusters. *D. cucullata* separated from *D. galeata* along PC1, which explained 7% of the variation. *D. longispina* separated from *D. galeata* and *D. cucullata* along PC2 which explained 6% of the variation (Figure 1B). Although sampled in different lakes, all parental species genotypes were grouped in tight clusters along the two axes with little evidence for population substructure. Population AR clustered with the *D. cucullata* reference individuals while population samples from DOB, EIC and SE were more spread out, mostly between the *D. galeata* and *D. longispina* clusters.

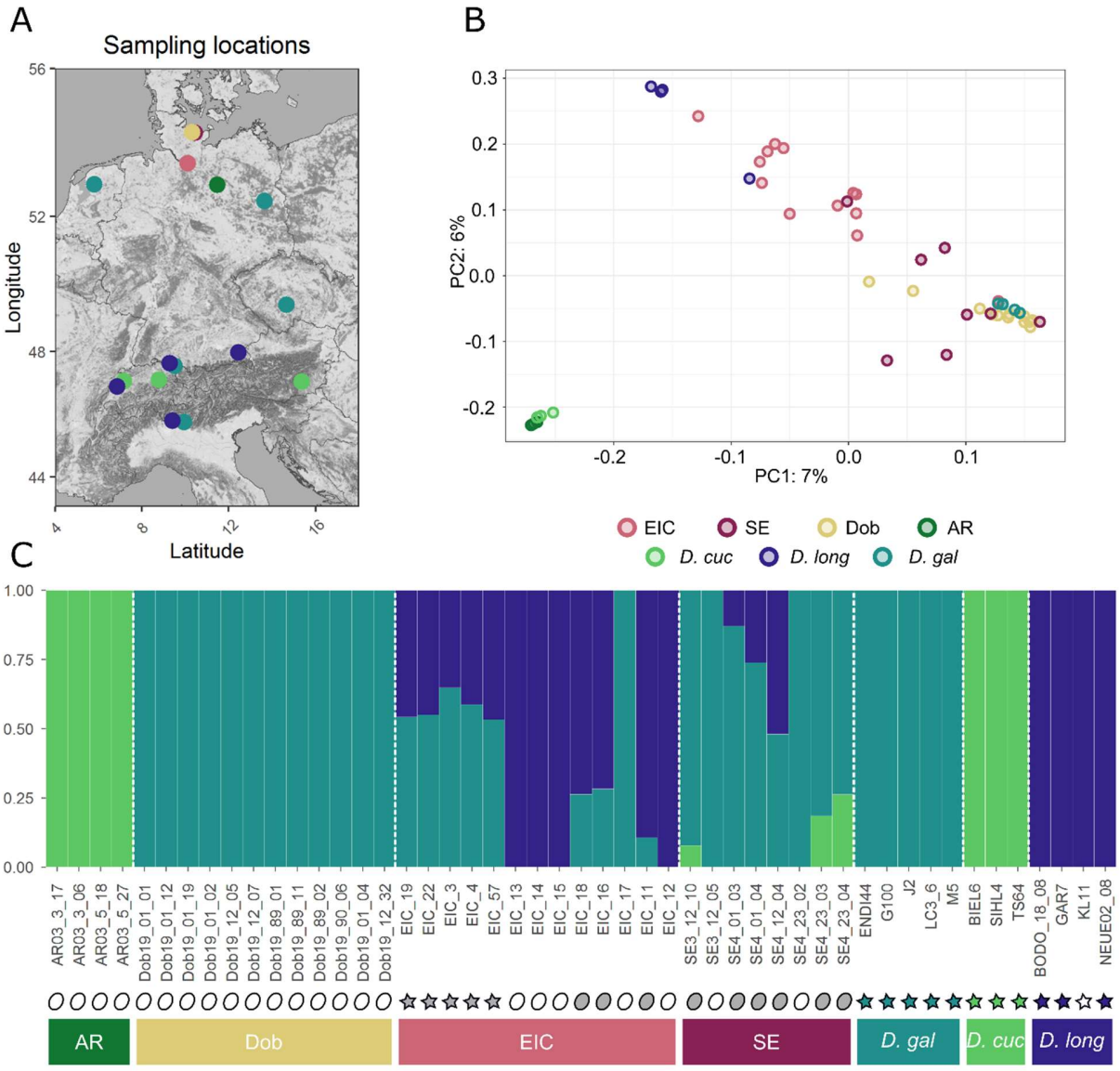

Figure 1: Parental species: *D. gal*: *D. galeata*, *D. long*: *D. longispina*, *D. cuc*; *D. cucullata*, populations: AR: Arendsee, Dob: Dobersdorfer See, SE: Selenter See, EIC: Eichbaumsee. Color coding is consistent throughout panels A and B **A.** Map of the sampling locations. **B.** PCA plot obtained with SNPrelate, including loci with linkage r^2 <0.5 within 500-kb sliding windows. **C.** Admixture plot obtained with K=3. Symbols indicate the sample type: oval for genotypes sequenced directly from resting eggs, stars for genotypes sampled in the water column and propagated clonally in the laboratory prior to sequencing. Symbol filling indicates how these genotypes were classified in subsequent analyses: white for non-admixed genotypes, grey for admixed genotypes, green, blue and teal for genotypes used as representatives for parental species. Bottom bars are color coded to match the color scheme used in panels A and B.

Admixture analyses uncover hybrids

The PCA results are confirmed by an admixture analysis conducted with ADMIXTURE (Alexander and Lange 2011) with K=3, supported by the lowest cross-validation error of the tested K values. The known

parental species genotypes were clearly separated into three clusters (Figure 1C). While we detect no evidence of admixture in the AR and DOB samples and, based on our parental species, consider them to belong to the species *D. cucullata* and *D. galeata*, respectively, the two other populations seem to consist mostly of admixed individuals. The five EIC samples sequenced after clonal propagation were all found to be admixed (*D. galeata* and *D. longispina*), while the EIC resting eggs were either admixed (3) or belonged to one of the parental species (5). SE resting eggs present all combinations of admixture except *D. cucullata* x *D. longispina*: *D. galeata* (2), admixed between *D. galeata* and *D. cucullata* (3), and admixed between *D. galeata* and *D. longispina* (3).

Ancestry painting

Based on results obtained in the ADMIXTURE analysis, two pairs of species and their putative hybrids were analyzed with an "ancestry painting" approach, outlined in Barth*, et al.* (2020) and Runemark*, et al.* (2018a): *D. galeata* and *D. longispina* parental genotypes and putative hybrids between them from populations EIC and SE, and *D. galeata* and *D. cucullata* parental genotypes and putative hybrids between them from population SE. Briefly, after identifying fixed sites for each of the species in the analyzed pair, heterozygosity was calculated for these sites and a hybrid index derived from the obtained results (https://github.com/mmatschiner/tutorials/tree/master/analysis_of_introgression_with_snp_data). Further, information on the maternal species is used to tentatively categorize the admixed individuals. For a first-generation hybrid (F1) the expectation would be 50% of the nuclear genome being derived from each parental species (hybrid index ≈ 0.5) and mostly heterozygous fixed sites (heterozygosity ≈ 1.0). Individuals originating from the backcrossing of F1 with one of the parental species are expected to have hybrid index values around 0.25 or 0.75. (Figure 2D). We consider individuals with intermediate hybrid indices (>0.25 and <0.75) and lower heterozygosity (<0.5) to be later-generation hybrids, meaning they have one or multiple hybrid ancestors we are not able to classify further (Slager*, et al.* 2020) We consider individuals with a hybrid index of ≤0.25 or ≥0.75 to be backcrossed with the respective parental species in at least one generation and the majority of the genome derives from one species. This definition is broad and will be refined with the addition of a greater number of parental genotypes.

The comparison of genotypes from parental species *D. galeata* and *D. longispina* (five and three individuals, respectively) allowed identifying a total of 335,052 fixed sites between the two species. Due to the quality filters applied to parental and hybrid genotypes, we could analyze 131,914 of these fixed sites in the putative hybrids, where read coverage was sufficient. The diploid genotypes were then plotted for all hybrids as homozygous for either of the parental species or as heterozygous (Figure 2A for the 50 longest scaffolds). The *D. longispina* reference clone KL11 was excluded from further analysis due to issues with missing data. All eleven genotypes from SE and EIC identified as likely *D. galeata* x *D. longispina* hybrids in the ADMIXTURE analysis possessed a *D. galeata* mitochondrial genome. The proportion of the maternal *D. galeata* genome in these hybrids, however, varied greatly, between 27.4% and 86.6%, and they all showed low heterozygosity, between 9.1% and 34.6% (Figure 2C, Table 2). These values are unlikely for F1 hybrids or backcrosses of F1 with one of the parental species (Table 2).

Comparing genotypes from the parental species *D. galeata* and *D. cucullata* (five and three individuals, respectively) led to identifying 715,438 fixed sites between the two species (due to quality filtering, 275,216 of these sites were further analyzed). All three *D. galeata* x *D. cucullata* hybrids carried a *D. cucullata* mitochondrial genome, their hybrid index varied between 0.079 and 0.267 and their heterozygosity ranged from 6.4% to 50.9 % (Figure 2B&C, Table 2). The individual SE_23_04 is most likely the result of a backcrossing with *D. galeata*; however, it is difficult to determine what backcrossed with it: either an F1 hybrid or a later generation hybrid i.e., that resulted from several generations of admixture. Haplotype information would be needed to gain certainty. The other two hybrids' lower hybrid index hints backcrossing with *D. galeata,* according to the criteria defined above.

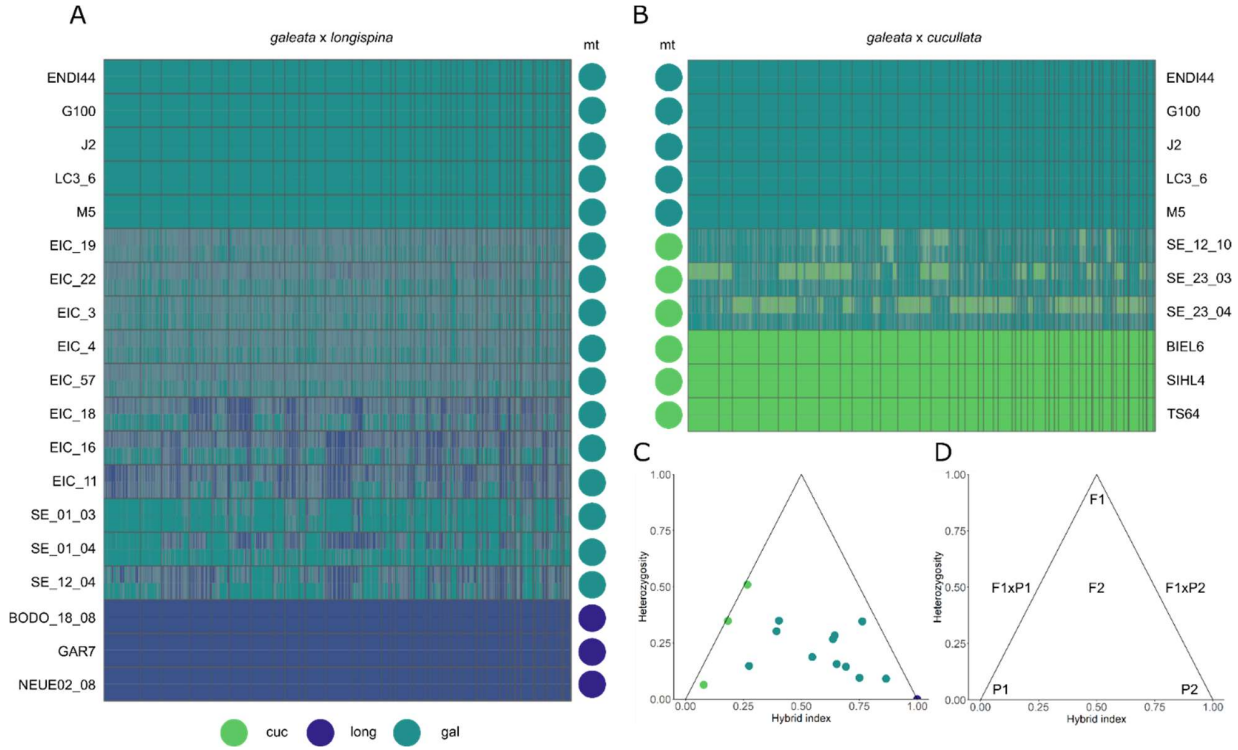

Figure 2 **Figure 3: Panels A & B** Ancestry painting of the hybrid individuals identified through the admixture analysis. Each row represents an individual. Colored circles on the side indicate the mitochondrial identity of the individuals, based on the analysis of full mitochondrial genomes. Scaffolds are sorted by length and separated by thin grey lines. In panels **A** and **B**, the five upper rows represent individuals assigned to the parental species *D. galeata*. In **A,** the last three rows correspond to individuals assigned to the parental species *D. longispina.* In **B.** the last three rows correspond to individuals assigned to the parental species *D. cucullata* Triangle plots summarizing **C.** the hybrid index and mitochondrial species identity for all individuals identified as admixed **D.** the hypothetical expected means of parental species (P1 and P2) and hybrid classes (F1xP1 and F1xP2: backcrosses with parental species P1 and P2, respectively).

Table 2: Data derived from ancestry painting analysis and based on the fixed sites inferred from analyzing parental species genotypes. Maternal species attribution is based on mitochondrial phylogeny, hybrid attribution is based on the ADMIXTURE plot.

Sample	Hybrid Index	Heterozygosity	Maternal species	Hybrid	Interpretation
SE_12_10	0.079	0.064	cuc	gal x cuc	Backcross gal
SE_23_03	0.183	0.348	cuc	gal x cuc	Backcross gal
SE_23_04	0.267	0.509	cuc	gal x cuc	Unclear
EIC_19	0.653	0.156	gal	gal x long	Later-generation
EIC_22	0.644	0.283	gal	gal x long	Later-generation
EIC_3	0.751	0.095	gal	gal x long	Backcross gal
EIC_4	0.693	0.144	gal	gal x long	Later-generation
EIC_57	0.637	0.267	gal	gal x long	Later-generation
EIC_18	0.393	0.302	gal	gal x long	Later-generation
EIC_16	0.403	0.349	gal	gal x long	Later-generation
EIC_11	0.274	0.148	gal	gal x long	Later-generation
SE_01_03	0.866	0.091	gal	gal x long	Backcross gal
SE_01_04	0.763	0.346	gal	gal x long	Backcross gal
SE_12_04	0.547	0.187	gal	gal x long	Later-generation

Population genomics parameters

To calculate genome-wide nucleotide diversity (π), between-taxon differentiation (F_{ST}), and between-taxon divergence (d_{xy}) within 100-kb sliding windows, we took advantage of the inference made with ADMIXTURE and pooled all genotypes which were unambiguously assigned to either of the parental species clusters. Consequently, a total of seven genotypes from four populations were classified as *D. cucullata*, eight from five populations as *D. longispina*, and 20 genotypes from eight populations as *D. galeata* (Table S2). All values (d_{xy}, π and F_{ST}) were calculated with the script popgenWindows.py (github.com/simonhmartin/genomics_general release 0.3) for each species pair and are plotted for the 50 largest scaffolds in Figure 3.

The window-based F_{ST} values for all three possible pairs among the three species averaged 0.274 for *D. galeata* vs *D. longispina*, 0.343 for *D. cucullata* vs *D. longispina* and 0.364 for *D. galeata* vs *D. cucullata*. The mean sequence divergence d_{xy} for the three pairs was 0.018 for *D. galeata* vs *D. longispina* and 0.022 for both *D. cucullata* vs *D. longispina* and *D. cucullata* vs *D. galeata*. Both parameters show similar

patterns, with lower values on average when comparing *D. galeata* to *D. longispina* than when comparing *cucullata* to either one of the other species. These patterns confirm the results obtained with other analyses, for example, the higher number of fixed sites between *D. galeata* and *D. cucullata* in the ancestry painting analysis.

The window-based estimates show high variability in levels of differentiation and divergence along the genome. Further, regions of high or low differentiation are mostly associated with depleted or high nucleotide diversity, respectively (see scaffolds 2 and 9 for example). However, the genome being represented by unordered scaffolds instead of chromosomes makes this difficult to interpret further.

Nucleotide diversity (π) to quantify the level of genetic variation within each taxon was on average higher for *D. longispina* (1.18%) than for the other two species (0.95% and 0.85% for *D. galeata* and *D. cucullata*, respectively). This cannot be explained by the differences in group sample sizes, since *D. galeata* was the group with the largest sample size (and highest number of sampled populations). To ensure our window-based estimates were not biased because of the overrepresentation of some populations in a group (e.g. DOB in the *galeata* group), we also calculated these indices using only one individual from each population per species; if one population contained multiple individuals, we picked one individual at random to represent this population (see Table S2 for a listing of the used genotypes - results shown in Figure S4).

Many more highly differentiated windows and genes were shared among two or all species pairs than would be expected by a random intersection (Figure S5). For example, a total of 2575 10kb windows had an F_{ST} value within the 95th percentile in the pair *D. galeata*/ *D. longispina* and 2569 in the pair *D. galeata*/ *D. cucullata*. The mean expected number of windows in common between these two pairwise comparisons was 113, but the number of windows in common observed in the data was 1601. A similar pattern was observed in all other intersections. This result suggests that the location of differentiated genome parts is not due to random processes but has biological significance. A GO-enrichment analysis of these isolated genes to shed light on the function of these species-specific genes, however, was not possible, because of the low number of genes with GO annotation. For the pair *D. galeata/cucullata*, only 12% of the genes in

346 the outlier windows were annotated with Gene Ontologies, for the pair *D. galeata/longispina* it was 11%
347 and for the *D. cucullata/longispina* pair it was 10%.

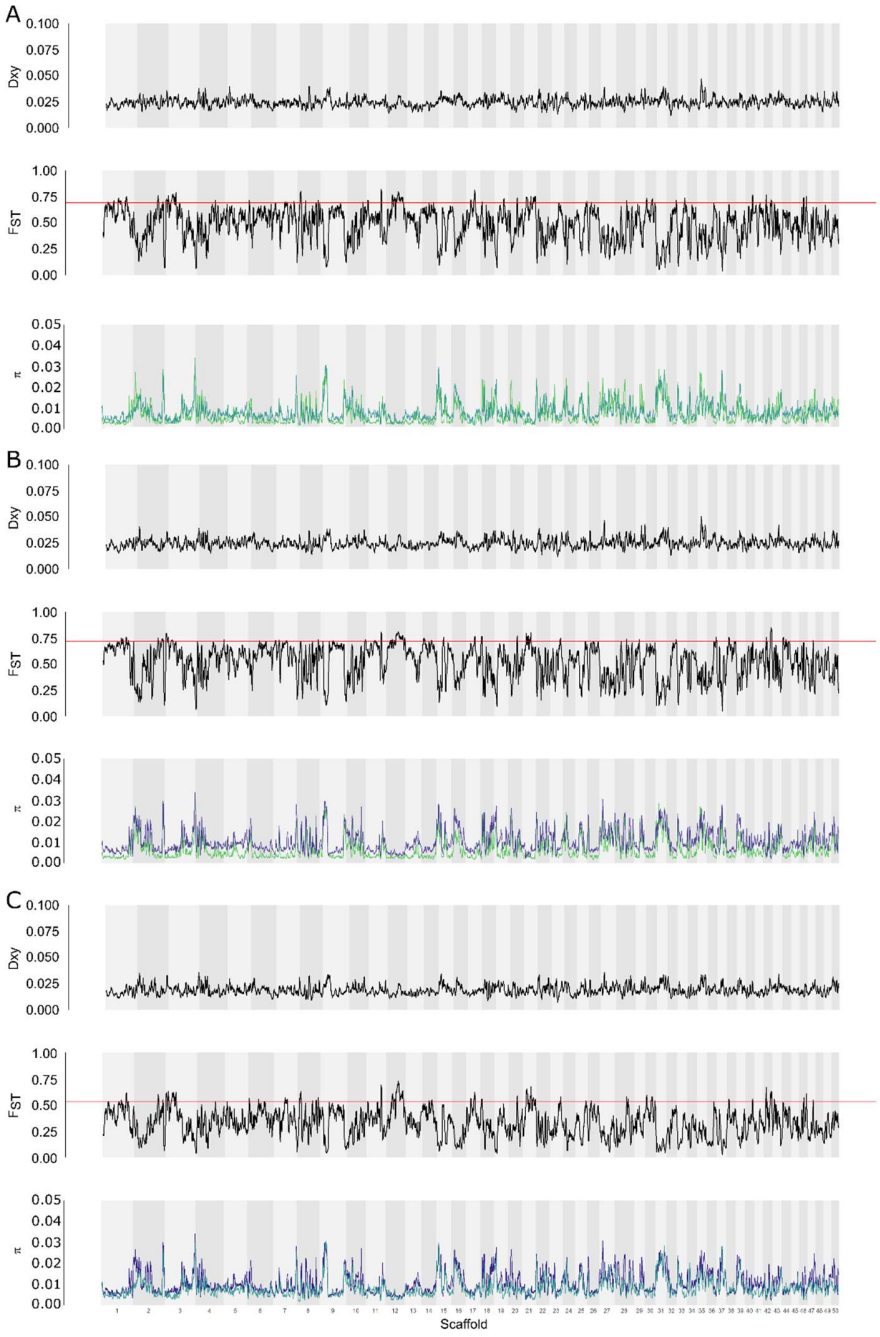

348

349 **Figure 4:** Window-based statistics for the pairs **A**. *D. galeata* / *D. cucullata,* **B**. *D cucullata* / *D. longispina* and **C**. *D.*
350 *galeata* / *D. longispina*, shown for the 50 largest scaffolds in 100kb windows with 10kb step size – calculations are for
351 all non-admixed individuals unambiguously assigned to parental species according to the ADMIXTURE analysis. **In**
352 **each panel from top to bottom:** d_{xy} values, pairwise F_{ST} values with a red horizontal line indicating the 95th percentile,
353 nucleotide diversity (π) for *D. galeata* (teal), *D. longispina* (dark blue), and *D. cucullata* (lime green).

Phylogeny based on complete mitochondrial genomes

Phylogenetic reconstruction based on the mitochondrial protein-coding and ribosomal RNA genes were largely consistent with earlier mitochondrial phylogenies based on single or few mitochondrial genes (e.g. Adamowicz*, et al.* 2009; Petrusek*, et al.* 2012). We identified highly supported clades comprising the respective parental genotypes, hence representing *D. longispina*, *D. cucullata*, and *D. galeata* mitochondrial haplotypes (Figure 4). *D. cucullata* and *D. galeata* mitochondrial haplotypes clustered as sister groups. While the mitochondrial haplotypes in the *D. longispina* and *D. cucullata* clusters do not show much divergence, the *D. galeata* haplotype cluster also contains deeper branching events (haplotype EIC_15 and AR3_17 / AR5_18). Further, although all samples from AR were unequivocally categorized as *D. cucullata* in the ADMIXTURE analysis and clustered with *D. cucullata* parental genotypes in the PCA, two of them have mitochondrial haplotypes falling into the *D. galeata* cluster (AR3_17 and AR5_18). A similar mismatch was also observed for EIC_15, which clusters with *D. longispina* when considering nuclear SNP and with *D. galeata* when considering the mitochondrial genome. Within the species clusters, we observed a grouping by lake with many haplotypes being either identical or very similar when originating from the same location. The trees obtained with either only protein-coding genes (CODON model) or protein-coding and ribosomal RNA genes but with a mixed model (DNA for rRNAs and CODON for DNA) were all consistent with the tree shown here and are therefore not included.

Patterns of introgression

We tested all four northern Germany populations (EIC, DOB, AR and SE) for admixture between the three reference species with f_3 statistics tests (Table 3) and considered a Z-score < -3 as significant (following Patterson*, et al.* 2012; Reich*, et al.* 2009). Negative and significant values (f_3=-0.19) using EIC as the test population and *D. galeata* and *D. longispina* as the source populations indicated mixed ancestry from these two or closely related populations. For population SE, the f_3 test supports both admixed ancestry from *D. galeata* and *D. longispina* (f_3=-0.09) and *D. galeata* and *D. cucullata* (f_3=-0.15). All tests for population DOB and AR were positive providing no evidence of admixture events. The supported introgression events

379 are consistent with the results in our previous analyses conducted with ADMIXTURE and the ancestry
380 painting approach.

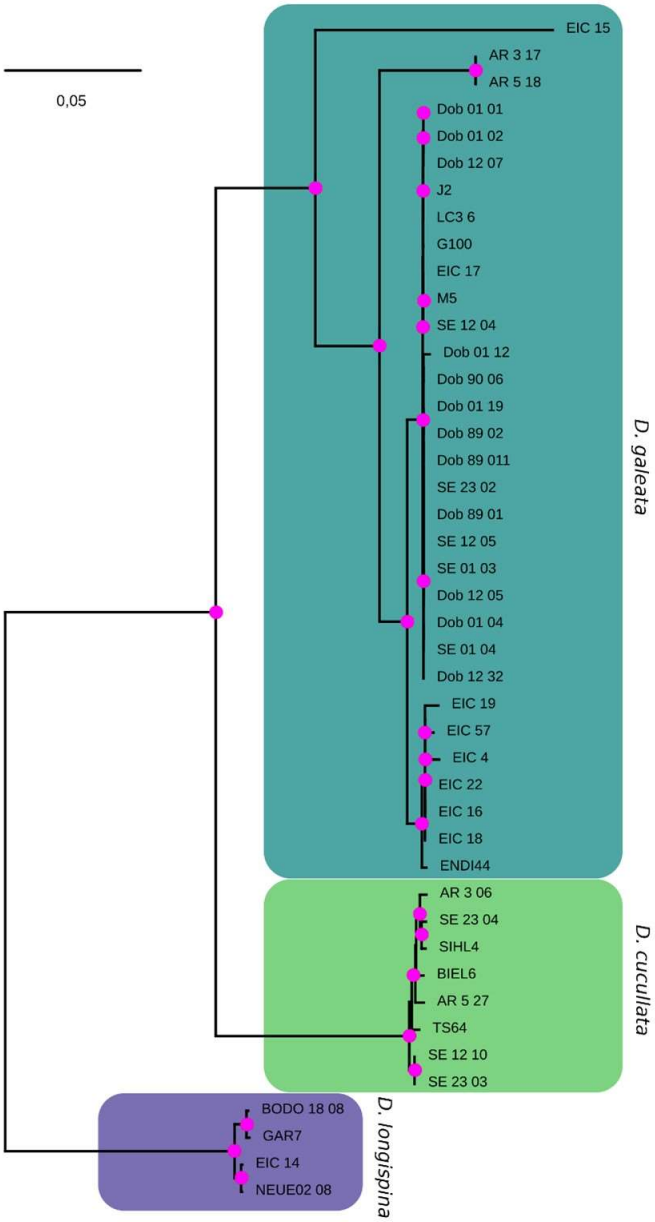

381

382 **Figure 5:** Maximum-likelihood tree reconstructed from mitochondrial protein-coding and ribosomal RNA genes of
383 parental species, clones sampled in the water column and resting eggs sequenced in this study. The tree reveals distinct
384 and highly supported clusters corresponding to *D. galeata*, *D. cucullata* and *D. longispina* mitotypes (as defined by
385 the respective parental species and a sister taxa relationship between *D. galeata* and *D. cucullata)*. Here, the best tree
386 (logL = -47950.82) rooted with outgroup *D. laevis* is depicted. Magenta dots indicate Shimodaira-Hasegawa
387 approximate likelihood ratio test values >= 80% and ultrafast bootstrap support values >= 95% calculated from 10,000
388 bootstrap replicates (SH-aLRT / UFboot). The scale bar corresponds to 0.05 nucleotide substitutions per nucleotide
389 site. KL11 was excluded due to missing data.

Table 3: Summary of the f_3 statistic for admixture in the form (C; A, B). A significantly (Z-score < -3, in bold) negative f_3 value implies that the target population C is admixed. SE: standard error

Source population A	Source population B	Target population C	f_3	SE	Z-score	# Sites
gal	long	AR	5.48226	0.154392	35.509	1,072,106
gal	cuc	AR	0.245124	0.006208	39.487	791,570
long	cuc	AR	0.225393	0.005475	41.165	875,293
gal	long	Dob	0.152725	0.003233	47.242	752,265
gal	cuc	Dob	0.150027	0.003028	49.546	815,035
long	cuc	Dob	1.763147	0.049657	35.506	1,059,418
gal	long	EIC	-0.193114	0.003224	**-59.898**	864,328
gal	cuc	EIC	0.086614	0.002623	33.025	1,119,715
long	cuc	EIC	0.014322	0.001774	8.071	1,145,530
gal	long	SE	-0.093233	0.003222	**-28.939**	1,029,744
gal	cuc	SE	-0.154696	0.003924	**-39.426**	955,516
long	cuc	SE	0.288212	0.011203	25.727	1,092,186

We performed local ancestry inference with Loter (Dias-Alves, *et al.* 2018) to trace genome-wide introgression among the hybrids and infer additional details about the parental species and backcross history from haplotype information. The results were summarized genome-wide for the ancestry proportion, heterozygosity of ancestry and the number of ancestry transitions where each ancestry tract is counted when the state of an SNP changes to the other species or at the end of a scaffold (Figure 5). The three *D. galeata* x *cucullata* hybrids were all found to have high *galeata* ancestry (73.9%-94.2%) and the individuals SE_23_03 and SE_23_04 were confirmed as the offspring of a later-generation hybrid and a pure *galeata* parent (Figure S6B).

Seven *D. galeata* x *longispina* hybrids had very high *galeata* ancestry (81.4%-97.9%), and visual inspection of the ancestry tracts (Figure S6A) revealed very short *longispina* tracts and scaffolds with multiple breakpoints indicating multiple generations of recombination. Four *D. galeata* x *longispina* hybrids had lower *galeata* ancestry (27.7%-59.0%) and the presence of complete *longispina* scaffolds implying some backcrossing with *longispina*. The haplotype phasing confirmed that the parents of all *D. galeata* x *longispina* hybrids were also of hybrid origin. The average and maximum ancestry tract length for all *D. galeata* x *longispina* hybrids is shorter than those for *D. galeata* x *cucullata* hybrids.

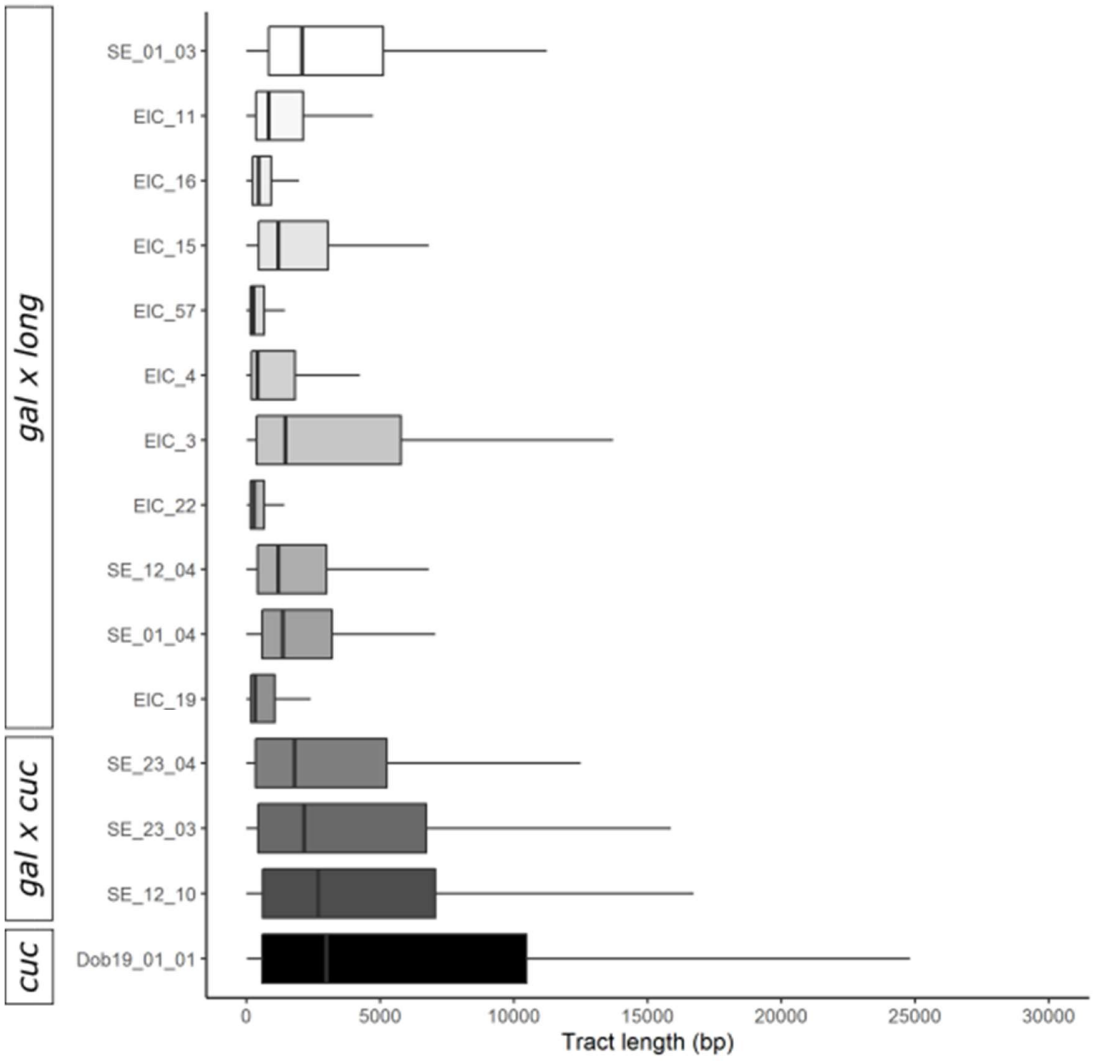

Figure 6: Distribution of the ancestry tract length where each ancestry tract represents the state of a SNP changing to the other species or the end of a scaffold in the local ancestry inference for each admixed individual and one non-admixed *D. cucullata* individual. The non-admixed individual displays the ancestry tract length distribution when all scaffolds derive from the same species. Hybrid type (according to ADMIXTURE analysis) is given on the left side.

Discussion

A reference genome for studying a species complex

Daphnia are a key species in freshwater habitats. Previous studies have established reference genomes for the model species *D. pulex* (Colbourne, *et al.* 2011; Ye, *et al.* 2017) and *D. magna* (Lee, *et al.* 2019). No high-quality reference genome for species belonging to the *Daphnia longispina* species complex was available so far. To date, it is unclear whether the ecological differenciation and/or intrinsic incompatibilities

drive and maintain divergence between DLSC species. Besides its utility for studies of hybridization events in the DLSC, the new assembly we present here will thus allow us to better understand the evolution of a key species in European freshwaters.

Even though the onset of the DLSC radiation was dated to 5-7 Mya based on nuclear and mitochondrial markers (Adamowicz*, et al.* 2009; Schwenk 1993; Taylor*, et al.* 1996), several factors confirm the suitability of this reference for all tested species. Mapping success and coverage of whole-genome data from *D. cucullata* and *D. longispina* to the reference genome were high, and we found no evidence of reference bias. This assembly clearly benefited from advances both in the sequencing technologies and assembly and post-processing algorithms since the first *Daphnia* genome (Colbourne*, et al.* 2011). The metrics used for assessing its quality reveal that in particular, the combination of long and short read technologies led to highly contiguous and accurate scaffolds. Although we likely did not recover the genome in its full length (133Mb out of an estimated 156Mb), and the N50 value is lower than those obtained for *D. pulex* (Ye*, et al.* 2017) and *D. magna* (Lee*, et al.* 2019), iterative scaffolding allowed for a very efficient gap-closing, and an exceptionally low number of mismatches, compared to the other *Daphnia* assemblies.

Pervasive introgression in the *Daphnia longispina* species complex

We utilize a method that allows us to interrogate biological archives and analyze whole *Daphnia* genomes directly from the resting egg bank (Lack*, et al.* 2018) without hatching and culturing several clonal lineages. This provides a wide sweep of populations, past and present, with each egg being the product of local sexual recombination.

While no evidence of introgression was found in the DOB population, the three other locations host a variety of admixed genotypes. SE & EIC can even be considered hybridization hotspots with more than 60% of individuals having hybrid ancestry, as revealed in the ADMIXTURE analysis. However, Kong and Kubatko (2021) very recently showed that ADMIXTURE is sensitive to unequal contributions by the parental species, and we thus sought to support these inferences by f_3 calculations and using an ancestry painting approach.

In DOB, ADMIXTURE delivered unequivocal results. Further, the f_3 index indicated that no introgression was detectable in this population. However, the PCA plot shows that some of the DOB genotypes are near hybrid individuals. ANGSD results are similar but these genotypes nearer the parental species (Figure S3A). To address these slightly contradictory results, we therefore conducted an ancestry painting on two DOB genotypes, (12_07 and 89_02, Table S7). Both genotypes had a very low heterozygosity, thus confirming the ADMIXTURE and f_3 outcomes. A possible explanation would be that these two genotypes carry variation that is not reflected in our limited sampling of the parental species. When comparing to microsatellite-based analysis including many more populations and data points (e.g. Thielsch*, et al.* 2009), the *D. galeata* cluster has often been larger and more diverse than the others. The seemingly two "stray" DOB genotypes are therefore likely well within the species variation boundaries. All mitochondrial haplotypes were clustered together in the phylogenetic reconstruction as well.

In AR, despite the high resting egg density found in the sediment, only very few could be successfully genotyped. While all inferences based on nuclear markers (PCA, ADMIXTURE, f_3) indicated an absence of hybridization or introgression in this population, the mitochondrial phylogenetic reconstruction showed diverging results. From a nuclear point of view, all genotypes could be categorized as *D. cucullata*, but two out of four AR individuals presented the mitochondrial genome of another species, i.e., *D. galeata*. However, the phylogenetic reconstruction shows that the two AR mitochondrial haplotypes form a cluster separate from the main *D. galeata* cluster, which hints at different evolutionary history for these mitochondrial genomes. Such distinct lineages within a species and mito-nuclear discordances were also found by Thielsch*, et al.* (2017) in the DLSC and mitochondrial capture has been detected in other *Daphnia* species (Marková*, et al.* 2013). It is an interesting phenomenon in the DLSC that merits to be further investigated in the future with broader sampling.

In EIC, both pelagic samples and resting eggs were analyzed. Genotypes sampled alive from the water column were all inferred to be admixed to various degrees, three resting egg samples were also admixed, and the remaining five were assigned to either one of the 2 parental species. We conducted the ancestry

469 painting approach on all EIC individuals; the fixed sites heterozygosity of the individuals categorized as
470 non-admixed in ADMIXTURE was indeed near zero (Table S7). Such high abundances of *D. galeata* x
471 *longispina* hybrid resting eggs in periods of rapidly changing environmental conditions (i.e. eutrophication)
472 have also been recorded in Lake Constance (Brede*, et al.* 2009). The high frequency of *D. galeata* x
473 *longispina* hybrids observed here might be due to similar ecological history: the lake Eichbaumsee was
474 created through sand excavation for construction work around ~40 years ago and is characterized by extreme
475 eutrophication and even hypertrophy that could not be remediated. The presence of later-generation hybrids
476 and backcrosses with *D. galeata* and *D. longispina* and short ancestry tract length suggest that both species
477 have been present and hybridizing for most of the lake's short history, or even that it was colonized by
478 individuals of hybrid origin. However, we only obtained contemporary samples for EIC and analysis of
479 resting eggs from sediment cores are needed to distinguish between the two hypotheses.

480 In SE, diversity is high, both in terms of species combinations in admixed individuals and in terms of degrees
481 of introgression. Although we analyzed eggs from sediments cores, they originated from the first centimeters
482 and there is, therefore, no clear temporal pattern that separates the different hybrid combinations found here.
483 Strikingly, while SE and DOB are geographically very close to each other (~10 km), and dispersal of resting
484 eggs through e.g., waterfowl or storms would be possible (Figuerola*, et al.* 2005; Frisch*, et al.* 2007; Pietrzak
485 and Slusarczyk 2006), the *Daphnia* communities are quite different. This might be due to their different
486 eutrophication levels, reflect the fact that initial colonization was followed by the establishment of different
487 species, or a combination of both. The observed diversity at such a small spatial scale underlines the mosaic
488 nature of freshwater habitats and the usefulness of approaches including many populations to fully
489 understand genetic diversity arising from colonization and hybridization events in the DLSC.

490 Previous studies using mitochondrial and few nuclear markers (e.g. Alric*, et al.* 2016; Thielsch*, et al.* 2012)
491 were able to categorize hybrids into F1, F2 and backcrosses. However, due to the low resolution of the used
492 markers, further categorizing and above all identification of genome-wide breaking points was not possible
493 at the time. The *D. galeata* reference genome and resequencing data offer now a much higher resolution to

494 assess later generation hybrids and patterns across the genome. In general, hybrids identified in this study
495 seem to have a complex history of multiple generations of hybridization and backcrossing with both parental
496 species that we are not able to detangle using only ancestry paintings. The local ancestry inference revealed
497 that the average ancestry tract length for *D. galeata* x *longispina* hybrids from EIC and SE is shorter than
498 those for *D. galeata* x *cucullata* hybrids. There are several explanations for the observed pattern. One is that
499 more generations of recombination led to shorter introgressed tracts, and the *D. galeata* x *longispina* hybrids
500 are therefore the result of a greater number of sexual generations than the *D. galeata* x *cucullata* hybrids.
501 The genomic mosaic of ancestry segments for all hybrid individuals is also characterized by multiple
502 breakpoints within the same scaffolds, which is only possible after multiple generations of recombination.
503 However, data on genome-wide recombination rates and selection are needed to reach solid conclusions
504 about the correlation between tract length and age of the hybridization event in the individual's ancestors.
505 Alternatively, reproductive isolation might be lower between *D. galeata* and *D. longispina* than between *D.*
506 *galeata* and *D. cucullata*, thus leading to faster introgression in the former case.

507 As evidenced by the comparison of genomic windows of higher divergence between species pairs, the
508 introgression pattern is not random: a given region exhibiting high F_{ST} values between the *D. galeata* and
509 *D. longispina* genotypes is also likely to show similarly high F_{ST} values in the *D. galeata*/ *D. cucullata* pair.
510 Further, some parts of the genome seem to be effectively shielded from introgression. About a quarter of all
511 genes (4136) are in regions that are highly differentiated between at least two species and about 5% (859)
512 in parts of the genome that are isolated among all three species of the complex. This is much more than
513 expected by chance (Figure S3) and is thus likely due to selection against introgression. It seems plausible
514 to search among these for genes that conserve the specific identity of the involved taxa, despite incomplete
515 reproductive isolation. Genes responsible for the observed ecological divergence among the taxa (Schwenk*,*
516 *et al.* 2000) or genetic incompatibilities are most likely candidates to be found in the observed divergent
517 regions. Given the ancient divergence, the speciation process in the DLSC might have attained a selection-
518 migration-drift equilibrium, for which there is growing empirical evidence in other species like stick insects
519 (Riesch*, et al.* 2017), flycatchers (Burri*, et al.* 2015), and non-biting midges (Schreiber and Pfenninger

520 2020). However, the current snapshot could equally likely be a consequence of one or several pulses of
521 hybridization. To assess the stability of the equilibrium, data showing that the introgression/selection
522 process is ongoing and constant across an extended period of time would be required and *Daphnia* offers
523 the unique opportunity to go back in time to test these alternative hypotheses.

524 ## New evidence for cytonuclear discordance

525 The genome-wide perspective also elucidated discordance between nuclear and mitochondrial patterns. The
526 phylogeny based on mitochondrial genomes conforms to previously inferred relationships in the DLSC and
527 suggests *D. galeata* and *D. cucullata* are sister species, with *D. longispina* as an outgroup (Adamowicz*, et*
528 *al.* 2009; Petrusek*, et al.* 2012). However, several of our analyses based on nuclear SNPs challenge this
529 view and suggest different evolutionary histories for mitochondrial and nuclear genomes. The ancestry
530 painting approach relies on the identification of fixed sites for species in a pairwise comparison. More sites
531 were found to be fixed between *D. galeata* and *D. cucullata* (715,438) than between *D. galeata* and *D.*
532 *longispina* (335,052), which implies a greater divergence between members of the former pair. Further, F_{ST}
533 values were on average higher between *D. galeata* and *D. longispina* (0.274) than between *D. galeata* and
534 *D. cucullata* (0.364). Reports of cytonuclear discordance are common both in plants (e.g. Folk*, et al.* 2017;
535 Huang*, et al.* 2014; Lee-Yaw*, et al.* 2019; Stephens*, et al.* 2015) and animals (e.g. Llopart*, et al.* 2014; Melo-
536 Ferreira*, et al.* 2014; Sarver*, et al.* 2021). Several processes can lead to this discordance among closely
537 related species: incomplete lineage sorting causing phylogenetic reconstructions based on mitochondrial
538 markers to differ from the true phylogeny of the taxa, or selection causing the fixation of different
539 mitochondrial genomes in different places from standing variation within species (e.g. Barrett and Schluter
540 2008). Alternatively, cytonuclear discordance may reflect hybridization between species and cytoplasmic
541 introgression, accompanied or not by selection (reviewed in Sloan*, et al.* 2017). The latter explanation would
542 be quite conceivable in the DLSC.

Conclusion

We here provide the first high-quality resources to study genome-wide patterns of divergence in the *Daphnia longispina* species complex, an ecologically important taxon in European freshwater habitats. By quantifying intra- and interspecific diversity, we provide a first glimpse into introgressive hybridization and lay the ground for further studies aiming at understanding how species boundaries are maintained in the face of gene flow.

Unlike for *D. pulex* and *D. magna*, no linkage groups are known for any species of the DLSC. Hi-C sequencing data will be added in the future to order scaffolds into larger, potentially chromosome-scale scaffolds. Such an approach holds promise in a species complex were laboratory crossings for F2 panels and traditional mapping are nearly impossible. This will allow discovering structural variants, identifying recombination breakpoints along each chromosome and thus provide a deeper understanding of the introgression patterns observed here. The functional role of genes in the regions of high divergence uncovered through this first analysis is yet unclear and will be addressed in future studies.

Finally, wider sampling, with the inclusion of more populations as well as more members of the species complex, and the reconstruction of a nuclear based phylogeny are necessary to reach conclusions about the species relationships and eventually identify the causes of the pattern uncovered here.

Materials & Methods

Sampling

The clonal line used for genome sequencing and assembly, M5, was hatched from a resting egg isolated from the upper layers (first 5cm, corresponding to the years 2000-2010) of a sediment core taken in Lake Müggelsee in 2010. Further, single genotypes representing the parental species from various locations were used in this study, henceforth “parental species genotypes”. Most of them were established from individuals sampled from the water column and are still maintained through asexual reproduction as monoclonal

cultures in the laboratory. Thus, all individuals of a clonal line are the same genotype and can be pooled to achieve sufficient amounts of genomic DNA. The species identity for these genotypes was established through a combination of methods: morphology, mitochondrial sequences, and nuclear markers.

Sediment cores were collected from Dobersdorfer See (DOB), Selenter See (SE) and Arendsee (AR), Germany using a gravity corer (Uwitec, Mondsee, AT) (Table S4). Samples were taken from the deepest part of the lakes to minimize past disturbance of the sediment. Cores were cut horizontally into 1cm layers and the layers were stored at 4 °C in the dark to prevent hatching. Sediment rate of the three lakes was determined using radioisotope dating (^{137}Cs and ^{210}Pb).

In addition, lake sediment from the shoreline of Eichbaumsee (EIC) (Table S4), Germany was collected by hand and stored at 4 °C. The exact age of the sediment is unknown but the upper layers most likely contain recent eggs from the last few years. Zooplankton samples were taken from Eichbaumsee using a plankton net (mesh size 150 µm) from which six *Daphnia* clonal lines were established in a laboratory setting with artificial medium (Aachener Daphnien Medium, ADaM Klüttgen*, et al.* 1994).

All sampling locations are plotted in Figure 1A and information on all samples is provided in Table S2.

Genome sequencing

DNA extraction for genome sequencing with Illumina & PacBio

DNA was extracted from around 60 clonal M5 individuals collected from batch cultures maintained in ADaM, and fed with the algae *Acutodesmus obliquus*, cultivated in medium modified after (Zehnder and Gorham 1960). Extraction was conducted following a phenol chloroform-based protocol with an RNase step and subsequently sequenced on an Illumina HiSeq4000 at BGI China. Additionally, tissue samples with around 3000 individuals were sent to BGI for DNA extraction and PacBio sequencing.

Re-sequencing (Population genomics approach)

DNA extraction from batch cultures for re-sequencing

For clonal lines used as reference for the parental species, individuals were raised in batch cultures and treated with antibiotics prior to collection and storage at -20 or -80°C. DNA was extracted with either a phenol chloroform method, a (modified) CTAB protocol or a rapid desalting method (MasterPure™ Complete DNA and RNA Purification Kit; Lucigen Corporation).

Total genomic DNA was isolated from 20 pooled adult *Daphnia* for each of the five EIC clonal lines using a CTAB extraction method (Doyle and Doyle 1987).

Whole Genome amplification on resting eggs for re-sequencing

To isolate *Daphnia* resting eggs from the sediment each sediment layer was sieved using a sieve with 125 µm mesh size and small amounts of the remaining sediment were resuspended in distilled water. Ephippia were eye spotted under a stereomicroscope, counted and transferred to 1.5 mL tubes. The water was removed and ephippia stored at -20 °C in the dark until further analysis.

The ephippia were then opened under a binocular with insect needles and tweezers previously treated under a clean bench (UV sterilization) and with DNase away (Thermo Fisher). Eggs that were already damaged, had an uneven shape or were orange, which is evidence for degradation, were discarded. The resting egg separated from the ephippial casing washed in 15 µl sterile 1x PBS and then transferred in 1 µl 1x PBS to a new tube with 2 µl fresh 1x PBS. The isolated eggs were stored at -80 ˚C at least overnight.

For whole genome amplification of single eggs, the REPLI-g Mini Kit (Qiagen) was used. This kit is enabling unbiased amplification of genomic loci via Multiple Displacement Amplification (MDA). The isolated resting eggs were thawed on ice and the whole genome was amplified following the manufacturer's protocol for amplification of genomic DNA from blood or cells. Briefly, denaturation buffer was added to the prepared resting eggs in 3 µl 1x PBS and amplified by REPLI-g Mini DNA Polymerase under isothermal conditions for 16 hours.

The amplified product was quantified on a Nanodrop spectrophotometer (Thermo Fisher) and with a Qubit Fluorometer (Thermo Fisher). Successful amplifications were purified with 0.4 x Agencourt AMPure XP magnetic beads (Beckman Coulter) to remove small fragments and eluted in 60 µl 1x TE buffer.

Fragments of the mitochondrial gene 16S rRNA gene were amplified to check successful amplification of *Daphnia* DNA using the universal cladoceran primers S1 and S2 (Schwenk, *et al.* 1998) and a low presence of bacterial DNA using universal primers for the bacterial 16S rDNA gene (Nadkarni, *et al.* 2002). Only samples with a successful amplification of the *Daphnia* 16S fragment and low amplification of the bacterial 16S fragment indicating low bacterial contamination were used for sequencing steps.

Library preparation and sequencing of re-sequencing samples

After quantification and quality control of the DNA using Nanodrop and Qubit instruments, libraries were prepared either directly in-house with the NEBNext® Ultra™ II DNA Library Prep Kit for Illumina® (New England Biolabs), or at the sequencing company Novogene (Cambridge, UK). Resequencing (paired-end 150bp reads) was then performed either at Novogene (UK) Company Limited or the Functional Genomics Center (ETH Zurich and University of Zurich) on Illumina NovaSeq 6000 and HiSeq4000 instruments.

Details on the procedure used for each sample are provided in Table S2.

Genome assembly and annotation

We provide here a summarized version of the procedure used to assemble and annotate the genome. Details can be found in Supplementary Methods.

Raw data QC

Illumina reads were trimmed and the adapter removed using a combination of Trimmomatic 0.38 (Bolger, *et al.* 2014), FastQC 0.11.7 (Andrews 2010) and MultiQC 1.6 (Ewels, *et al.* 2016) within autotrim 0.6.1 (Waldvogel, *et al.* 2018). To filter out reads possibly originating from contamination from known sources (see below), a FastQ Screen like approach was chosen. In brief, the reads are separated by results of mapping behavior to different genomes. Positive controls consisted of genome data for other *Daphnia* species

636 (dmagna-v2.4 and Daphnia_pulex_PA42_v3.0, see Supplementary Methods for accession numbers), and
637 negative control i.e. sequences deemed undesirable for genome assembly consisted of genome data from
638 human, bacteria, viruses and the algae used to feed the batch cultures. The resulting database comprised
639 108,163 sequences (total sequence space 42.2 Gb). Both Illumina reads and PacBio subreads were mapped
640 against the database with NextGenMap (Sedlazeck*, et al.* 2013) and minimap2 (Li 2018), respectively.

641 Reads did only pass the filtering if they either did not map to the database at all or had at least one hit against
642 one of the two *Daphnia* genomes. Table 2 in Supplementary methods gives an overview of the effect of
643 different filtering steps.

644 ### Assembly and contamination screening

645 All paired and unpaired contamination filtered Illumina reads as well as the contamination filtered PacBio
646 reads were used as input for RA 0.2.1 (https://github.com/rvaser/ra). Blobtools 1.0 (Laetsch and Blaxter
647 2017) was used to screen the resulting assembly for possible unidentified contamination in the hybrid
648 assembly. Briefly, bwa mem 0.7.17 (Li 2013) was used to map Illumina reads back to the assembly and
649 taxonomic assignment was done by sequence similarity search with blastn 2.9.0+ (Camacho*, et al.* 2009).
650 Contamination with different bacteria was clearly identifiable, and contigs with coverage below 10x and/or
651 GC content above 50% were removed. Additionally, PacBio reads mapping to these contigs were removed
652 to minimize false scaffolding in further steps. The contig corresponding to the mitochondrial genome was
653 identified after a blast search against available mitochondrial genomes for this species and removed from
654 the assembly.

655 ### Scaffolding and gap closing

656 The blobtools filtered PacBio reads were used for scaffolding and gapclosing, which was conducted in three
657 iterations. Each iteration consisted of a scaffolding step with SSPACE LongRead 1-1 (Boetzer and Pirovano
658 2014), a gap closing step with LR Gapcloser (https://github.com/CAFS-bioinformatics/LR_Gapcloser;
659 commit 156381a), and a step to polish former gap parts with short reads using bwa mem 0.7.17-r1188 and

660 Pilon 1.23 (Walker, *et al.* 2014) in a pipeline developed to this effect, wtdbg2-racon-pilon.pl 0.4
661 (https://github.com/schellt/wtdbg2-racon-pilon).

662 ### Assembly quality assessment

663 Contiguity was analyzed with Quast 5.0.2 (Gurevich, *et al.* 2013) at different stages of the assembly process.
664 Further, mapping rate, coverage and insert size distribution were assessed by mapping Illumina and PacBio
665 reads with bwa mem and Minimap 2.17 respectively. To show absence of contamination in the assembly
666 blobtools was ran as above. The genome size was estimated by dividing the mapped nucleotides by the
667 mode of the coverage distribution of the Illumina reads by backmap 0.3
668 (https://github.com/schellt/backmap), resulting in 156.86Mb (with the obtained assembly length amounting
669 to 85% of this estimated length). Additionally, the genome size was estimated using a k-mer based approach
670 by creating a histogram from raw Illumina reads with Jellyfish 1.1.12 (Marçais and Kingsford 2011) and
671 running the GenomeScope web application (http://qb.cshl.edu/genomescope/) resulting in a genome size
672 estimate of 150.6Mb.

673 Completeness in terms of single copy core orthologs of the final scaffolds was assessed with BUSCO 3.0.2
674 (Simão, *et al.* 2015), using the Arthropoda set (odb9).

675 ### Genome Annotation

676 RepeatModeler 2.0 (Smit and Hubley 2015) was run to identify *D. galeata* specific repeats. The 1,115
677 obtained repeat families were combined with 237 *D. pulex* and 1 *D. pulicaria* repeat sequences from
678 RepBase release 20181026 to create the final repeat library. The genome assembly was then soft masked
679 with RepeatMasker 4.1.0 (Smit, *et al.* 2013-2015), resulting in 21.9% of the assembly being masked.

680 Gene prediction models were produced with Augustus 3.3.2 (Stanke, *et al.* 2008), GeneMark ET
681 4.48_3.60_lic (Lomsadze, *et al.* 2005) and SNAP 2006-07-28 (Korf 2004). The Augustus model was based
682 on the soft masked assembly and the *D. galeata* transcriptome (HAFN01.1, Huylmans, *et al.* 2016). The
683 GeneMark model was obtained by first mapping trimmed RNAseq reads to the assembly with HISAT 2.1.0

(Kim, *et al.* 2019) and then processing the resulting bam file with bam2hints and filterIntronsFindStrand.pl from Augustus to create a gff file with possible introns, which was finally fed into GeneMark.

The structural annotation was conducted in MAKER 2.31.10 (Holt and Yandell 2011). Briefly, the unmasked genome assembly, the species own transcriptome assembly as ESTs, the complete Swiss-Prot 2019_10 (UniProt Consortium, 2019) and the protein sequences resulting from *D. magna* (Lee, *et al.* 2019), as well as *D. pulex* (Ye, *et al.* 2017) genome annotations as protein evidence, were used as input for MAKER. In total three iterations of MAKER with retraining of the Augustus and SNAP model in between the iterations were conducted.

The quality of the structural annotation was assessed by comparing values as number of genes, gene space, etc. to existing annotations for other *Daphnia* genomes. Furthermore, core orthologs from BUSCO's Arthropoda (odb9) set and conserved domain arrangements from the Arthropoda reference set of DOGMA 3.4 (Dohmen, *et al.* 2016) were searched in the annotated protein set.

The functional annotation was conducted using InterProScan 5.39-77.0 (Jones, *et al.* 2014) as well as a blast against the Swiss-Prot 2019_10.

Population samples

Raw data QC and contamination check

The quality of raw reads was checked using FastQC v0.11.5. Adapter trimming and quality filtering were performed using Trimmomatic v0.36 with the following parameters: ILLUMINACLIP:TruSeq3-PE.fa:2:30:10 TRAILING:20 SLIDINGWINDOW:4:15 MINLEN:70. For samples sequenced on a NovaSeq6000 instrument and presenting a typical polyG tail, the program fastp (Chen, *et al.* 2018) was used for trimming as well. To assess contamination in the WGA samples FastQ Screen v0.14.0 with the bwa mapping option was used (Wingett and Andrews 2018). A custom database was built to map trimmed reads against possible contaminants that included general common contaminants such as *Homo sapiens*, the UniVec reference database, a bacterial and a viral reference set as well as the *D. galeata* genome and

Acutodesmus obliquus draft genome (see Supplementary Methods for accession numbers). Samples with <25 % reads mapped to the *D. galeata* genome (and 25% contamination) were excluded from further analysis because the whole amplification of the resting egg most likely failed.

Mapping to reference genome and variant calling

The variant calling was performed within the Genome Analysis Toolkit (GATK v4.1.4.0; McKenna*, et al.* 2010) program according to GATK4 best practices (Van der Auwera*, et al.* 2013). The trimmed reads were mapped to the *D. galeata* genome using the BWA-MEM algorithm in BWA v0.7.17 with the -M parameter and adding read group identifiers for Picard compatibility (Li and Durbin 2009). PCR duplicates were marked and filtered out in the BAM file using Picard v2.21.1 (http://broadinstitute.github.io/picard/).

To call variants for each sample GATK HaplotypeCaller in GATK was used with the --emitRefConfidence GVCF option resulting in a genomic variant call format (gVCF) file with information on each position for each individual (Poplin*, et al.* 2018). All gVCF files were consolidated using CombineGVCFs and joint genotyping was performed with GenotypeGVCFs. The VCF file was filtered to include only SNPs and hard filtering was performed to remove variants with a QualByDepth <10, StrandOddsRatio >3, FisherStrand >60, mapping quality <40, MappingQualityRankSumTest <-8 and ReadPosRankSumTest <-5.

Subsequently, we removed sites with either very high coverage (>450) or for which genotypes were missing for more than 20% of the individuals using VCFtools v0.1.5 (Danecek*, et al.* 2011). The final SNP data set for downstream analyses included 3,240,339 SNPs across the 49 samples.

In addition, GenotypeGVCFs was run with the --include-non-variant-sites option to output all variant as well as invariant genotyped sites. The final invariant data set included 127,530,229 sites after removing indels and multi-allelic sites with BCFtools v1.9 (Li 2011) and is used for population genomic analysis to be able to calculate the total number of genotyped sites (variant and invariant) within a genomic window.

As we mapped all different species to the reference *D. galeata* genome we assessed possible reference bias by checking the distribution of reference and alternative alleles observed at heterozygous genotypes based

on Pinsky, *et al.* (2021). We pooled all genotypes which were unambiguously assigned to either of the parental species clusters *D. galeata*, *D. cucullata* and *D. longispina* as was done for the population genomic parameters (Table S2) or classified as hybrids using ADMIXTURE inference. Without reference bias, we would expect that in heterozygous genotypes the reference and the alternative allele are on average represented by 50% of the reads. An indication of reference bias would be that the *D. galeata* reference allele would be more frequent.

Phylogenetic and population genetics inferences

Mitochondrial genome assemblies and phylogenetic analyses

All reads were used to produce mitochondrial genome assemblies using the "de novo assembly" and "find mitochondrial scaffold" modules provided in MitoZ v2.4 with default settings (Meng, *et al.* 2019). For some samples, this was not sufficient and we used two approaches to recover a complete mitogenome: either the mitochondrial baiting and iterative mapping implemented in MITObim v1.9.1 (Hahn, *et al.* 2013) with the *D. galeata* mitochondrial reference genome or the modified baiting and iterative mapping in GetOrganelle v1.7.1 (Jin, *et al.* 2020) with the animal database and k-mer values set to 21, 45, 65, 85 and 105. The procedure used for each dataset is given in Table S5.

We annotated the mitochondrial genome assemblies with the mitochondrial annotation web server MITOS2 (Bernt, *et al.* 2013) using the mitochondrial codon code 05 for invertebrates. Automated genome annotation identified thirteen protein-coding genes (PCGs), two ribosomal RNA genes (rRNAs), and twenty-two transfer RNA genes (tRNAs). Initially, the mitochondrial genes (PCGs and rRNAs, Table S6) were individually aligned with MUSCLE v3.8.1551 (Edgar 2004) and visually checked for their quality. The mitochondrial genome assemblies with discrepancies, i.e., a lot of missing data and/or split features were excluded from further analysis. The final data set (Table S6) included 44 mitochondrial genomes from this study and the previously published mitochondrial genome of *Daphnia laevis* (Martins Ribeiro, *et al.* 2019/, accession number: NC_045243.1/, accession number: NC_045243.1). The mitochondrial genes of the final data set were individually realigned with MUSCLE v3.8.1551 (Edgar 2004) and MACSE v2.05 (Ranwez,

et al. 2018) and concatenated into a mitochondrial DNA matrix (Table S6) using SequenceMatrix v1.8.1 (Vaidya, *et al.* 2011). During this step, we used MACSE v2.05 to realign PCG genes keeping the information about codon position (gene partitioning) and to remove STOP codons. The final dataset consisted of the concatenation matrix of the thirteen protein-coding (PCGs) and the two structural ribosomal RNA (rRNAs) genes. With this alignment, phylogenetic trees were reconstructed using IQ-TREE v1.6.12 (Nguyen, *et al.* 2015). We initially partitioned the alignment into a full partition model, i.e., each gene and all three codon positions for PCGs, and then ran IQ-TREE with partition analyses (-spp, Chernomor, *et al.* 2016), ModelFinder (- m MFP+MERGE, Kalyaanamoorthy, *et al.* 2017) and 10,000 ultrafast bootstrap (-bb 10000, Hoang, *et al.* 2018) and SH-like approximate likelihood ratio test (-alrt 10000, Guindon, *et al.* 2010) replicates. The resulting trees were visualized in R (R Core Team 2017) using the multifunctional phylogenetics package phytools (Revell 2012).

Ancestry and population structure

A principal component analysis was conducted in R v3.6.2 (R Core Team 2017) with the package SNPRelate v1.20.1 (Zheng, *et al.* 2012). Linkage disequilibrium (LD) was calculated within a 500-kb sliding window and LD-pruned for r^2 values >0.5 before conducting the PCA for all sites using the snpgdsPCA function with default settings. The relative large LD value was chosen because clonal reproduction and the overlap of generations due to diapause leads to increased linkage disequilibrium in *Daphnia* (Brede, *et al.* 2009).

Genetic admixture was estimated using ADMIXTURE v1.3.0 (Alexander and Lange 2011). The SNP set VCF file was converted to BED format using plink v1.90b6.13 (Chang, *et al.* 2015). The log-likelihood values were estimated for one to five genetic clusters (K) of ancestral populations and admixture analysis were run for the most appropriate K value with 10-fold cross-validation. We also conducted the PCA and Admixture analysis using PCAngsd implemented in ANGSD and NgsAdmix, respectively (Korneliussen, *et al.* 2014) to take genotype likelihoods into account (details in Supplementary methods). The results did not differ substantially and are shown in Figure S3.

782 However, using such a population genetic clustering approach to estimate ancestry coefficients is not
783 directly equivalent to the proportion of hybrid ancestry in each individual and should be interpreted with
784 caution (Kong and Kubatko 2021; Lawson, *et al.* 2018). The results of the ADMIXTURE analysis suggested
785 that the dataset included hybrids between *D. longispina* and *D. galeata* as well as *D. cucullata* and *D.*
786 *galeata*. We then followed the "ancestry painting" procedure outlined in Barth, *et al.* (2020) and Runemark,
787 *et al.* (2018b), and classified sites according to their F_{ST} values when comparing parental species sets. Unlike
788 the PCA and the admixture analysis, this approach requires the user to define parental genotypes; the
789 individuals belonging to these sets are indicated with stars in Figure 1C. Fixed sites are those where a
790 specific allele is fixed in all individuals belonging to one parental species and another allele fixed in the
791 other parental species. To show the ancestry of the hybrid individuals each fixed site was plotted in an
792 "ancestry painting" if at least 80% of genotypes were complete using available ruby scripts
793 (https://github.com/mmatschiner/tutorials/tree/master/analysis_of_introgression_with_snp_data). These
794 scripts calculate the heterozygosity of each individual and visualize regions that are possibly affected by
795 introgression. The mitochondrial genome assembly from each individual was used to determine the maternal
796 species and the proportion of the genome derived from the maternal species was then calculated for each
797 hybrid. For gal x cuc hybrids the hybrid index scale ranges from 0 (gal) to 1 (cuc) and for gal x long hybrids
798 from 0 (long) to 1 (gal).

799 ### Window-based population parameters

800 To assess genome-wide genetic differentiation between the clusters identified with admixture, we calculated
801 nucleotide diversity (π), between-taxon differentiation (F_{ST}), and between-taxon divergence (d_{xy}) using the
802 Python script popgenWindows.py (github.com/simonhmartin/genomics_general release 0.3, Martin, *et al.*
803 2020) with a sliding 100-kb window, a step size of 10kb and at least 20kb genotyped sites within each
804 window. To compare species pairs we only considered individuals assigned to parental species based on
805 ADMIXTURE results (Table S2). In addition, we also calculated these parameters using one randomly
806 chosen individual from each population per species to check if the estimates are biased because of the
807 overrepresentation of some populations in a species group (Table S2).

Sets of outlier windows were defined as those with F_{ST} values in the upper 95th percentile of the distribution for each of the 3 pairwise comparisons. Further, the genes in these windows were extracted using the annotation file. We used a randomization approach to assess whether the observed intersections (i.e. outlier F_{ST} windows occurring in both species) between all seven possible species comparisons are larger or smaller than expected by chance. For this, we randomly drew the observed number of windows, respectively genes from the total number of 10kb windows in the assembly (13,330), respectively the total number of annotated genes (15,845) without replacement and calculated the intersections for all possible comparisons. We compared the resulting intersections from 1,000 replicates with the observed values (Figure S5).

Inferring introgression

To identify admixture among three populations we calculated the f_3 statistic with ADMIXTOOLS v 7.0 (Patterson*, et al.* 2012) implemented in the admixr package in R (Petr*, et al.* 2019). We used two parental source populations (A and B) and the target population (C) in the form (C; A, B). Significantly negative f_3 statistic indicates that population C is a mixture of populations A and B or closely related populations.

Local ancestry inference

To prepare the SNP set, Beagle v4.1 was used to phase and impute genotypes with 10,000 bp step size and 1000 bp overlapping sliding windows (Browning and Browning 2009). Local ancestry inference was conducted with Loter (Dias-Alves*, et al.* 2018) which infers the origin of each SNP in an admixed individual from two ancestral source populations and doesn't require additional biological parameters. The respective two parental species populations were used to reconstruct the ancestry tracts of the three putative *galeata* x *cucullata* hybrid individuals and eleven putative *galeata* x *longispina* hybrid individuals using Loter with default settings.

Authors contributions

MC, JN, AT, SD and MHM performed the sampling and wet lab work. TS, JN and AT conducted the genome assembly and annotation. JN conducted the population genomic analysis and mitochondrial genome

832 reconstruction. TH and MHM conducted the phylogenetic analyses. JN, TS, MC, MP, MHM and TH wrote
833 the manuscript, and all authors edited and contributed to the final version. All authors gave final approval
834 for preprint deposition and publication.

835 Data Availability

836 Genome assembly, annotation and read data (Illumina and PacBio) for the genotype M5 are stored under
837 accession number PRJEB42807. Short read data from resequencing are available in the European
838 Nucleotide Archive under accession numbers ERS5080327- ERS5080375, ERS4993274 and ERS4993282.
839 The annotation used in the present analysis is deposited in Zenodo (DOI: 10.5281/zenodo.4479324),
840 together with supplementary information on the mitochondrial tree (alignment file).

841 Acknowledgments

842 We thank LOEWE-TBG for providing sequencing funds. TH and MM were supported by the grant
843 “SeeWandel: Life in Lake Constance - the past, present and future” within the framework of the Interreg V
844 programme “Alpenrhein-Bodensee-Hochrhein (Germany/Austria/Switzerland/Liechtenstein)”, which
845 funds are provided by the European Regional Development Fund as well as the Swiss Confederation and
846 cantons. MHM was supported by the Austrian Science Fund (FWF): P29667-B25 and J 3774. The funders
847 had no role in study design, data collection and analysis, decision to publish, or preparation of the
848 manuscript. The computational results presented here have been achieved in (part) using the LEO HPC
849 infrastructure of the University of Innsbruck. Some of the data produced and analyzed in this paper were
850 generated in collaboration with the Genetic Diversity Centre (GDC), ETH Zurich.

851 We thank Jae-Seong Lee and Zhiqiang Ye for giving us access to genome annotations for *Daphnia magna*
852 (SK strain) and *Daphnia pulex* (PA42 strain), respectively. Miklós Bálint provided sediment samples and
853 isotope data for the Arendsee lake. We thank Michael Matschiner for his help with ancestry painting and
854 two anonymous reviewers for their comments on a previous version of the manuscript.

References

Abbott R, *et al.* 2013. Hybridization and speciation. J. Evol. Biol. 26: 229-246. doi: 10.1111/j.1420-9101.2012.02599.x

Adamowicz SJ, Petrusek A, Colbourne JK, Hebert PDN, Witt JDS 2009. The scale of divergence: A phylogenetic appraisal of intercontinental allopatric speciation in a passively dispersed freshwater zooplankton genus. Mol. Phylogenet. Evol. 50: 423-436. doi: 10.1016/j.ympev.2008.11.026

Alexander DH, Lange K. 2011. Enhancements to the ADMIXTURE algorithm for individual ancestry estimation. BMC Bioinform. 12: 246

Alric B, *et al.* 2016. Local human pressures influence gene flow in a hybridizing *Daphnia* species complex. J. Evol. Biol. 29: 720-735. doi: 10.1111/jeb.12820

Andrews S. 2010. FastQC: A quality control tool for high throughput sequence data.

Arnold ML, Martin NH 2009. Adaptation by introgression. J. Biol. 8.

Barrett RD, Schluter D 2008. Adaptation from standing genetic variation. Trends Ecol. Evol. 23: 38-44.

Barth JM, *et al.* 2020. Stable species boundaries despite ten million years of hybridization in tropical eels. Nat. Commun. 11: 1-13.

Barton NH, Hewitt GM 1985. Analysis of hybrid zones. Annu. Rev. Ecol. Syst. 16: 113-148.

Beaton MJ, Hebert PD 1994. Variation in chromosome numbers of *Daphnia* (Crustacea, Cladocera). Hereditas 120: 275-279.

Bernt M, *et al.* 2013. MITOS: improved de novo metazoan mitochondrial genome annotation. Mol. Phylogenet. Evol. 69: 313-319.

Billiones R, Brehm M, Klee J, Schwenk K 2004. Genetic identification of Hyalodaphnia species and interspecific hybrids. Hydrobiologia 526: 43-53.

Boetzer M, Pirovano W 2014. SSPACE-LongRead: scaffolding bacterial draft genomes using long read sequence information. BMC Bioinform. 15: 211.

Bolger AM, Lohse M, Usadel B 2014. Trimmomatic: a flexible trimmer for Illumina sequence data. Bioinformatics 30: 2114-2120. doi: 10.1093/bioinformatics/btu170

Brede N, *et al.* 2009. The impact of human-made ecological changes on the genetic architecture of *Daphnia* species. P Natl Acad Sci USA 106: 4758-4763. doi: 10.1073/pnas.0807187106

Brede N, *et al.* 2006. Microsatellite markers for European *Daphnia*. Mol. Ecol. Notes 6: 536-539. doi: 10.1111/j.1471-8286.2005.01218.x

Browning BL, Browning SR 2009. A unified approach to genotype imputation and haplotype-phase inference for large data sets of trios and unrelated individuals. Am. J. Hum. Genet. 84: 210-223.

Burri R, *et al.* 2015. Linked selection and recombination rate variation drive the evolution of the genomic landscape of differentiation across the speciation continuum of *Ficedula* flycatchers. Genome Res. 25: 1656-1665.

890 Butlin RK, *et al.* 2014. Parallel evolution of local adaptation and reproductive isolation in the face of gene
891 flow. Evolution 68: 935-949.

892 Camacho C, *et al.* 2009. BLAST+: architecture and applications. BMC Bioinform. 10: 421.

893 Canestrelli D, *et al.* 2017. Climate change promotes hybridisation between deeply divergent species. PeerJ
894 5: e3072

895 Chang CC, *et al.* 2015. Second-generation PLINK: rising to the challenge of larger and richer datasets.
896 Gigascience 4: s13742-015-0047-8

897 Chen S, Zhou Y, Chen Y, Gu J 2018. fastp: an ultra-fast all-in-one FASTQ preprocessor. Bioinformatics
898 34: i884-i890.

899 Chernomor O, Von Haeseler A, Minh BQ 2016. Terrace aware data structure for phylogenomic inference
900 from supermatrices. Syst. Biol. 65: 997-1008.

901 Colbourne JK, *et al.* 2011. The Ecoresponsive Genome of *Daphnia pulex*. Science 331: 555-561. doi:
902 10.1126/science.1197761

903 Cordellier M, Wojewodzic MW, Wessels M, Kuster CJ, Von Elert E. 2021. Next-generation sequencing of
904 DNA from resting eggs: signatures of eutrophication in a lake's sediment. Zoology 145: 125895 doi:
905 10.1016/j.zool.2021.125895

906 Cornetti L, Fields PD, Van Damme K, Ebert D 2019. A fossil-calibrated phylogenomic analysis of *Daphnia*
907 and the Daphniidae. Mol. Phylogenet. Evol. 137: 250-262.

908 Cousyn C, *et al.* 2001. Rapid, local adaptation of zooplankton behavior to changes in predation pressure in
909 the absence of neutral genetic changes. P Natl Acad Sci USA 98: 6256-6260. doi: 10.1073/pnas.111606798

910 Danecek P, *et al.* 2011. The variant call format and VCFtools. Bioinformatics 27: 2156-2158.

911 Dias-Alves T, Mairal J, Blum MG 2018. Loter: A software package to infer local ancestry for a wide range
912 of species. Mol. Biol. Evol. 35: 2318-2326.

913 Dlouha S, *et al.* 2010. Identifying hybridizing taxa within the *Daphnia longispina* species complex: a
914 comparison of genetic methods and phenotypic approaches. Identifying hybridizing taxa within the *Daphnia*
915 *longispina* species complex: a comparison of genetic methods and phenotypic approaches 643: 107-122.
916 doi: DOI 10.1007/s10750-010-0128-8

917 Doellman MM, *et al.* 2018. Genomic differentiation during speciation-with-gene-flow: Comparing
918 geographic and host-related variation in divergent life history adaptation in *Rhagoletis pomonella*. Genes 9:
919 262.

920 Dohmen E, Kremer LP, Bornberg-Bauer E, Kemena C 2016. DOGMA: domain-based transcriptome and
921 proteome quality assessment. Bioinformatics 32: 2577-2581.

922 Doyle JJ, Doyle JL 1987. A rapid DNA isolation procedure for small quantities of fresh leaf tissue.
923 Phytochem. Bull. 19: 11-15.

924 Dziuba MK, *et al.* 2020. Temperature increase altered *Daphnia* community structure in artificially heated
925 lakes: a potential scenario for a warmer future. Sci. Rep. 10: 13956

926 Edgar RC 2004. MUSCLE: Multiple sequence alignment with high accuracy and high throughput. Nucleic
927 Acids Res 32: 1792-1797. doi: 10.1093/nar/gkh340

928 Ewels P, Magnusson M, Lundin S, Käller M 2016. MultiQC: summarize analysis results for multiple tools
929 and samples in a single report. Bioinformatics 32: 3047-3048.

930 Figuerola J, Green AJ, Michot TC 2005. Invertebrate eggs can fly: evidence of waterfowl-mediated gene
931 flow in aquatic invertebrates. Am. Nat. 165: 274-280.

932 Flaxman SM, Wacholder AC, Feder JL, Nosil P 2014. Theoretical models of the influence of genomic
933 architecture on the dynamics of speciation. Mol. Ecol. 23: 4074-4088.

934 Folk RA, Mandel JR, Freudenstein JV 2017. Ancestral gene flow and parallel organellar genome capture
935 result in extreme phylogenomic discord in a lineage of angiosperms. Syst. Biol. 66: 320-337.

936 Fraïsse C, Roux C, Welch JJ, Bierne N 2014. Gene-flow in a mosaic hybrid zone: is local introgression
937 adaptive? Genetics 197: 393-951.

938 Frisch D, Green AJ, Figuerola J 2007. High dispersal capacity of a broad spectrum of aquatic invertebrates
939 via waterbirds. Aquat. Sci. 69: 568-574.

940 Frisch D*, et al.* 2014. A millennial-scale chronicle of evolutionary responses to cultural eutrophication in
941 *Daphnia*. Ecol. Lett. 17: 360-368. doi: 10.1111/ele.12237

942 Gannon JE, Stemberger RS 1978. Zooplankton (Especially Crustaceans and Rotifers) as Indicators of Water
943 Quality. Trans. Am. Microsc. Soc. 97: 16-35. doi: 10.2307/3225681

944 Gliwicz ZM. 1990. Why do cladocerans fail to control algal blooms? In. Biomanipulation Tool for Water
945 Management: Springer. p. 83-97.

946 Griebel J, Gießler S, Yin M, Wolinska J 2016. Parental and hybrid *Daphnia* from the *D. longispina* complex:
947 long-term dynamics in genetic structure and significance of overwintering modes. J. Evol. Biol. 29: 810-
948 823.

949 Guindon S*, et al.* 2010. New algorithms and methods to estimate maximum-likelihood phylogenies:
950 assessing the performance of PhyML 3.0. Syst. Biol. 59: 307-321.

951 Gurevich A, Saveliev V, Vyahhi N, Tesler G 2013. QUAST: quality assessment tool for genome assemblies.
952 Bioinformatics 29: 1072-1075.

953 Hahn C, Bachmann L, Chevreux B. 2013. Reconstructing mitochondrial genomes directly from genomic
954 next-generation sequencing reads—a baiting and iterative mapping approach. Nucleic Acids Res 41: e129

955 Harrison RG 1986. Pattern and process in a narrow hybrid zone. Heredity 56: 337-349.

956 Herrmann M, Henning-Lucass N, Cordellier M, Schwenk K 2017. A genotype–phenotype association
957 approach to reveal thermal adaptation in *Daphnia galeata*. A genotype–phenotype association approach to
958 reveal thermal adaptation in *Daphnia galeata* 327: 53-65. doi: 10.1002/jez.2070

959 Hoang DT, Chernomor O, Von Haeseler A, Minh BQ, Vinh LS 2018. UFBoot2: improving the ultrafast
960 bootstrap approximation. Mol. Biol. Evol. 35: 518-522.

961 Holt C, Yandell M. 2011. MAKER2: an annotation pipeline and genome-database management tool for
962 second-generation genome projects. BMC Bioinform. 12: 491

963 Huang DI, Hefer CA, Kolosova N, Douglas CJ, Cronk QC 2014. Whole plastome sequencing reveals deep
964 plastid divergence and cytonuclear discordance between closely related balsam poplars, *Populus*
965 *balsamifera* and *P. trichocarpa* (Salicaceae). New Phytol. 204: 693-703.

966 Huylmans AK, López Ezquerra A, Parsch J, Cordellier M 2016. De Novo Transcriptome Assembly and
967 Sex-Biased Gene Expression in the Cyclical Parthenogenetic *Daphnia galeata*. Genome Biol. Evol 8: 3120-
968 3139. doi: 10.1093/gbe/evw221

969 Jin J-J*, et al.* 2020. GetOrganelle: a fast and versatile toolkit for accurate de novo assembly of organelle
970 genomes. Genome Biol. 21: 1-31.

971 Jones P*, et al.* 2014. InterProScan 5: genome-scale protein function classification. Bioinformatics 30: 1236-
972 1240.

973 Kaiser TS, von Haeseler A, Tessmar-Raible K, Heckel DG 2021. Timing strains of the marine insect *Clunio*
974 *marinus* diverged and persist with gene flow. Mol. Ecol. n/a. doi: 10.1111/mec.15791

975 Kalyaanamoorthy S, Minh BQ, Wong TK, von Haeseler A, Jermiin LS 2017. ModelFinder: fast model
976 selection for accurate phylogenetic estimates. Nat. Methods 14: 587-589.

977 Keller B, Wolinska J, Manca M, Spaak P 2008. Spatial, environmental and anthropogenic effects on the
978 taxon composition of hybridizing *Daphnia*. Philos. Trans. R. Soc. Lond. B Biol. Sci. 363: 2943-2952. doi:
979 10.1098/rstb.2008.0044

980 Kim D, Paggi JM, Park C, Bennett C, Salzberg SL 2019. Graph-based genome alignment and genotyping
981 with HISAT2 and HISAT-genotype. Nat. Biotechnol. 37: 907-915.

982 Klüttgen B, Dülmer U, Engels M, Ratte HT 1994. ADaM, an artificial freshwater for the culture of
983 zooplankton. Water Res. 28: 743-746.

984 Kong S, Kubatko LS 2021. Comparative Performance of Popular Methods for Hybrid Detection using
985 Genomic Data. Syst. Biol. 70: 891–907. doi: 10.1093/sysbio/syaa092

986 Korf I. 2004. Gene finding in novel genomes. BMC Bioinform. 5: 59

987 Korneliussen TS, Albrechtsen A, Nielsen R. 2014. ANGSD: analysis of next generation sequencing data.
988 ANGSD: analysis of next generation sequencing data 15: 356

989 Lack JB, Weider LJ, Jeyasingh PD 2018. Whole genome amplification and sequencing of a *Daphnia* resting
990 egg. Mol. Ecol. Resour.: 1-10. doi: 10.1111/1755-0998.12720

991 Laetsch DR, Blaxter ML. 2017. BlobTools: Interrogation of genome assemblies. F1000Research: 6:1287

992 Lampert W, Sommer U. 2007. Limnoecology: The Ecology of Lakes and Streams. Oxford: Oxford
993 University Press.

994 Lawson DJ, Van Dorp L, Falush D 2018. A tutorial on how not to over-interpret STRUCTURE and
995 ADMIXTURE bar plots. A tutorial on how not to over-interpret STRUCTURE and ADMIXTURE bar plots
996 9: 1-11.

997 Lee-Yaw JA, Grassa CJ, Joly S, Andrew RL, Rieseberg LH 2019. An evaluation of alternative explanations
998 for widespread cytonuclear discordance in annual sunflowers (*Helianthus*). New Phytol. 221: 515-526.

999 Lee B-Y*, et al.* 2019. The genome of the freshwater water flea *Daphnia magna*: A potential use for
1000 freshwater molecular ecotoxicology. Aquat. Toxicol. 210: 69-84.

1001 Li H. 2013. Aligning sequence reads, clone sequences and assembly contigs with BWA-MEM. arXiv:
1002 1303.3997

1003 Li H 2018. Minimap2: pairwise alignment for nucleotide sequences. Bioinformatics 34: 3094-3100.

1004 Li H 2011. A statistical framework for SNP calling, mutation discovery, association mapping and population
1005 genetical parameter estimation from sequencing data. Bioinformatics 27: 2987-2993.

1006 Li H, Durbin R 2009. Fast and accurate short read alignment with Burrows–Wheeler transform.
1007 Bioinformatics 25: 1754-1760.

1008 Limburg PA, Weider LJ 2002. 'Ancient'DNA in the resting egg bank of a microcrustacean can serve as a
1009 palaeolimnological database. P Roy Soc B-Biol Sci 269: 281-287.

1010 Llopart A, Herrig D, Brud E, Stecklein Z 2014. Sequential adaptive introgression of the mitochondrial
1011 genome in *Drosophila yakuba* and *Drosophila santomea*. Mol. Ecol. 23: 1124-1136.

1012 Lomsadze A, Ter-Hovhannisyan V, Chernoff YO, Borodovsky M 2005. Gene identification in novel
1013 eukaryotic genomes by self-training algorithm. Nucleic Acids Res 33: 6494-6506.

1014 Ma X, Hu W, Smilauer P, Yin M, Wolinska J 2019. *Daphnia galeata* and *D. dentifera* are geographically
1015 and ecologically separated whereas their hybrids occur in intermediate habitats: A survey of 44 Chinese
1016 lakes. Mol. Ecol. 28: 785-802.

1017 Marçais G, Kingsford C 2011. A fast, lock-free approach for efficient parallel counting of occurrences of k-
1018 mers. A fast, lock-free approach for efficient parallel counting of occurrences of k-mers 27: 764-770.

1019 Marková S, Dufresne F, Manca M, Kotlík P. 2013. Mitochondrial capture misleads about ecological
1020 speciation in the *Daphnia pulex* complex. PLoS ONE 8: e69497

1021 Martin SH*, et al.* 2013. Genome-wide evidence for speciation with gene flow in *Heliconius* butterflies.
1022 Genome Res. 23: 1817-1828.

1023 Martin SH, Davey JW, Salazar C, Jiggins CD. 2019. Recombination rate variation shapes barriers to
1024 introgression across butterfly genomes. PLoS Biol. 17: e2006288 doi: 10.1371/journal.pbio.2006288

1025 Martin SH*, et al.* 2020. Whole-chromosome hitchhiking driven by a male-killing endosymbiont. Whole-
1026 chromosome hitchhiking driven by a male-killing endosymbiont 18: e3000610

1027 Martins Ribeiro M*, et al.* 2019. Mitogenome of *Daphnia laevis* (Cladocera, Daphniidae) from Brazil.
1028 Mitochondrial DNA Part B 4: 194-196.

1029 McKenna A*, et al.* 2010. The Genome Analysis Toolkit: A MapReduce framework for analyzing next-
1030 generation DNA sequencing data. Genome Res. 20: 1297-1303. doi: 10.1101/gr.107524.110

1031 Meier JI*, et al.* 2017. Ancient hybridization fuels rapid cichlid fish adaptive radiations. Nat. Commun. 8: 1-
1032 11.

1033 Melo-Ferreira J*, et al.* 2014. The elusive nature of adaptive mitochondrial DNA evolution of an arctic
1034 lineage prone to frequent introgression. Genome Biol. Evol 6: 886-896.

1035 Meng G, Li Y, Yang C, Liu S. 2019. MitoZ: a toolkit for animal mitochondrial genome assembly, annotation
1036 and visualization. Nucleic Acids Res 47: e63

1037 Miner BE, De Meester L, Pfrender ME, Lampert W, Hairston NG 2012. Linking genes to communities and
1038 ecosystems: Daphnia as an ecogenomic model. P Roy Soc B-Biol Sci 279: 1873-1882. doi:
1039 10.1098/rspb.2011.2404

1040 Möst MH 2013. Environmental change and its impact on hybridising Daphnia species complexes. [Doctoral
1041 Thesis]. [Zürich]: ETH.

1042 Nadkarni MA, Martin FE, Jacques NA, Hunter N 2002. Determination of bacterial load by real-time PCR
1043 using a broad-range (universal) probe and primers set. Microbiology 148: 257-266. doi: 10.1099/00221287-
1044 148-1-257

1045 Nguyen L-T, Schmidt HA, Von Haeseler A, Minh BQ 2015. IQ-TREE: a fast and effective stochastic
1046 algorithm for estimating maximum-likelihood phylogenies. Mol. Biol. Evol. 32: 268-274.

1047 Orsini L*, et al.* 2013. The evolutionary time machine: using dormant propagules to forecast how populations
1048 can adapt to changing environments. Trends Ecol. Evol. 28: 274-282. doi: 10.1016/j.tree.2013.01.009

1049 Patterson N*, et al.* 2012. Ancient admixture in human history. Genetics 192: 1065-1093.

1050 Petr M, Vernot B, Kelso J 2019. admixr—R package for reproducible analyses using ADMIXTOOLS.
1051 Bioinformatics 35: 3194-3195.

1052 Petrusek A*, et al.* 2008a. A taxonomic reappraisal of the European *Daphnia longispina* complex (Crustacea,
1053 Cladocera, Anomopoda). Zool. Scr. 37: 507-519. doi: 10.1111/j.1463-6409.2008.00336.x

1054 Petrusek A, Seda J, Machacek J, Ruthova S, Smilauer P 2008b. *Daphnia* hybridization along ecological
1055 gradients in pelagic environments: the potential for the presence of hybrid zones in plankton. Philos. Trans.
1056 R. Soc. Lond. B Biol. Sci. 363: 2931-2941. doi: 10.1098/rstb.2008.0026

1057 Petrusek A, Thielsch A, Schwenk K 2012. Mitochondrial sequence variation suggests extensive cryptic
1058 diversity within the Western Palearctic *Daphnia longispina* complex. Limnol Oceanogr 57: 1838-1845. doi:
1059 10.4319/lo.2012.57.6.1838

1060 Pietrzak B, Slusarczyk M 2006. The fate of the ephippia - *Daphnia* dispersal in time and space. Pol. J. Ecol.
1061 54: 709-714.

1062 Pinsky ML*, et al.* 2021. Genomic stability through time despite decades of exploitation in cod on both sides
1063 of the Atlantic. Genomic stability through time despite decades of exploitation in cod on both sides of the
1064 Atlantic 118.

1065 Poplin R*, et al.* 2018. Scaling accurate genetic variant discovery to tens of thousands of samples. Scaling
1066 accurate genetic variant discovery to tens of thousands of samples: 201178 doi: 10.1101/201178

1067 Rafajlović M, Emanuelsson A, Johannesson K, Butlin RK, Mehlig B 2016. A universal mechanism
1068 generating clusters of differentiated loci during divergence-with-migration. Evolution 70: 1609-1621.

1069 Ranwez V, Douzery EJ, Cambon C, Chantret N, Delsuc F 2018. MACSE v2: toolkit for the alignment of
1070 coding sequences accounting for frameshifts and stop codons. Mol. Biol. Evol. 35: 2582-2584.

1071 Reich D, Thangaraj K, Patterson N, Price AL, Singh L 2009. Reconstructing Indian population history.
1072 Nature 461: 489-494.

1073 Rellstab C, Keller B, Girardclos S, Anselmetti FS, Spaak P 2011. Anthropogenic eutrophication shapes the
1074 past and present taxonomic composition of hybridizing *Daphnia* in unproductive lakes. Science 56: 292-
1075 302. doi: 10.4319/lo.2011.56.1.0292

1076 Revell LJ 2012. phytools: an R package for phylogenetic comparative biology (and other things). Methods
1077 Ecol. Evol. 3: 217-223.

1078 Riesch R, *et al.* 2017. Transitions between phases of genomic differentiation during stick-insect speciation.
1079 Nat. Ecol. Evol. 1: 82

1080 Runemark A, Eroukhmanoff F, Nava-Bolanos A, Hermansen JS, Meier JI 2018a. Hybridization, sex-
1081 specific genomic architecture and local adaptation. Hybridization, sex-specific genomic architecture and
1082 local adaptation 373. doi: 10.1098/Rstb.2017.0419

1083 Runemark A, *et al.* 2018b. Variation and constraints in hybrid genome formation. Nat. Ecol. Evol. 2: 549-
1084 556. doi: 10.1038/s41559-017-0437-7

1085 Rusek J, *et al.* 2015. New possibilities arise for studies of hybridization: SNP-based markers for the multi-
1086 species *Daphnia longispina* complex derived from transcriptome data. J. Plankton Res. 37: 626-635. doi:
1087 10.1093/plankt/fbv028

1088 Sarver BA, *et al.* 2021. Diversification, Introgression, and Rampant Cytonuclear Discordance in Rocky
1089 Mountains Chipmunks (Sciuridae: *Tamias*). Syst. Biol.

1090 Schreiber D, Pfenninger M 2020. Genomic divergence landscape in recurrently hybridizing *Chironomus*
1091 sister taxa suggests stable steady state between mutual gene flow and isolation. Evol. Lett. 5: 86-100.

1092 Schwenk K 1993. Interspecific hybridization in *Daphnia*: distinction and origin of hybrid matrilines. Mol.
1093 Biol. Evol. 10: 1289-1302.

1094 Schwenk K, Bijl M, Menken SBJ 2001. Experimental interspecific hybridization in *Daphnia*. Hydrobiologia
1095 442: 67-73. doi: 10.1023/A:1017594325506

1096 Schwenk K, Posada D, Hebert PDN 2000. Molecular systematics of European Hyalodaphnia: the role of
1097 contemporary hybridization in ancient species. P Roy Soc B-Biol Sci 267: 1833-1842. doi:
1098 10.1098/rspb.2000.1218

1099 Schwenk K, *et al.* 1998. Genetic markers, genealogies and biogeographic patterns in the cladocera. Aquat.
1100 Ecol 32: 37-51.

1101 Sedlazeck FJ, Rescheneder P, Von Haeseler A 2013. NextGenMap: fast and accurate read mapping in highly
1102 polymorphic genomes. Bioinformatics 29: 2790-2791.

1103 Seidendorf B, Boersma M, Schwenk K 2007. Evolutionary stoichiometry: The role of food quality for clonal
1104 differentiation and hybrid maintenance in a *Daphnia* species complex. Limnol Oceanogr 52: 385-394.

1105 Simão FA, Waterhouse RM, Ioannidis P, Kriventseva EV, Zdobnov EM 2015. BUSCO: assessing genome
1106 assembly and annotation completeness with single-copy orthologs. Bioinformatics 31: 3210-3212. doi:
1107 10.1093/bioinformatics/btv351

1108 Skage M, *et al.* 2007. Intra-specific rDNA-ITS restriction site variation and an improved protocol to
1109 distinguish species and hybrids in the *Daphnia longispina* complex. Hydrobiologia 594: 19-32. doi:
1110 10.1007/s10750-007-9090-5

1111 Slager DL, *et al.* 2020. Cryptic and extensive hybridization between ancient lineages of American crows.
1112 Mol. Ecol. 29: 956-969.

1113 Sloan DB, Havird JC, Sharbrough J 2017. The on-again, off-again relationship between mitochondrial
1114 genomes and species boundaries. Mol. Ecol. 26: 2212-2236.

1115 Smit AFA, Hubley R. 2015. RepeatModeler Open. Version 1.0.

1116 Smit AFA, Hubley R, Green P. 2013-2015. RepeatMasker Open-4.0.

1117 Spaak P 2004. Spatial and temporal patterns of sexual reproduction in a hybrid *Daphnia* species complex.
1118 Spatial and temporal patterns of sexual reproduction in a hybrid *Daphnia* species complex 26: 625-635. doi:
1119 10.1093/plankt/fbh064

1120 Spaak P, Fox J, Hairston NG 2012. Modes and mechanisms of a *Daphnia* invasion. P Roy Soc B-Biol Sci
1121 279: 2936-2944. doi: 10.1098/rspb.2012.0280

1122 Spaak P, Hoekstra JR 1997. Fish predation on a *Daphnia* hybrid species complex: A factor explaining
1123 species coexistence? Limnol Oceanogr 42: 753-762. doi: 10.4319/lo.1997.42.4.0753

1124 Stanke M, Diekhans M, Baertsch R, Haussler D 2008. Using native and syntenically mapped cDNA
1125 alignments to improve de novo gene finding. Bioinformatics 24: 637-644.

1126 Stephens JD, Rogers WL, Mason CM, Donovan LA, Malmberg RL 2015. Species tree estimation of diploid
1127 *Helianthus* (Asteraceae) using target enrichment. Am. J. Bot. 102: 910-920.

1128 Taylor DJ, Hebert PDN, Colbourne JK 1996. Phylogenetics and evolution of the *Daphnia longispina* group
1129 (Crustacea) based on 12S rDNA sequence and allozyme variation. Mol. Phylogenet. Evol. 5: 495-510. doi:
1130 10.1006/mpev.1996.0045

1131 Team RC. 2017. R: A Language and Environment for Statistical Computing: R Foundation for Statistical
1132 Computing, Vienna, Austria.

1133 Thielsch A, Brede N, Petrusek A, De Meester L, Schwenk K 2009. Contribution of cyclic parthenogenesis
1134 and colonization history to population structure in *Daphnia*. Mol. Ecol 18: 1616-1628. doi: 10.1111/j.1365-
1135 294X.2009.04130.x

1136 Thielsch A, Knell A, Mohammadyari A, Petrusek A, Schwenk K. 2017. Divergent clades or cryptic species?
1137 Mito-nuclear discordance in a *Daphnia* species complex. BMC Evol. Biol. 17: 227

1138 Thielsch A, Volker E, Kraus RHS, Schwenk K 2012. Discrimination of hybrid classes using cross-species
1139 amplification of microsatellite loci: methodological challenges and solutions in *Daphnia*. Mol. Ecol. Resour.
1140 12: 697-705. doi: 10.1111/j.1755-0998.2012.03142.x

1141 Tollrian R, Harvell CD. 1999. The ecology and evolution of inducible defenses: Princeton University Press.

1142 Trentini M 1980. Chromosome numbers of nine species of Daphniidae (Crustacea, Cladocera). Genetica
1143 54: 221-223.

1144 Vaidya G, Lohman DJ, Meier R 2011. SequenceMatrix: concatenation software for the fast assembly of
1145 multi-gene datasets with character set and codon information. Cladistics 27: 171-180.

1146 Van der Auwera GA*, et al.* 2013. From FastQ data to high-confidence variant calls: the genome analysis
1147 toolkit best practices pipeline. Curr. Protoc. Bioinformatics 43: 11-10.

1148 Vergilino R, Markova S, Ventura M, Manca M, Dufresne F 2011. Reticulate evolution of the *Daphnia pulex*
1149 complex as revealed by nuclear markers. Mol. Ecol. 20: 1191-1207.

1150 Waldvogel AM*, et al.* 2018. The genomic footprint of climate adaptation in *Chironomus riparius*. Mol.
1151 Ecol. 27: 1439-1456.

1152 Walker BJ*, et al.* 2014. Pilon: an integrated tool for comprehensive microbial variant detection and genome
1153 assembly improvement. PLoS ONE 9: e112963

1154 Wingett SW, Andrews S 2018. FastQ Screen: A tool for multi-genome mapping and quality control.
1155 F1000Research 7.

1156 Wolf HG. 1987. Interspecific hybridization between *Daphnia hyalina*, *D. galeata*, and *D. cucullata* and
1157 seasonal abundances of these species and their hybrids. In: Forró L., D.G. F, editors. Cladocera. Dordrecht:
1158 Springer. p. 213-217.

1159 Wolf HG, Mort MA 1986. Interspecific hybridization underlies phenotypic variability in *Daphnia*
1160 populations. Oecologia 68: 507-511.

1161 Ye ZQ*, et al.* 2017. A New Reference Genome Assembly for the Microcrustacean *Daphnia pulex*. G3 7:
1162 1405-1416. doi: 10.1534/g3.116.038638

1163 Yeaman S, Whitlock MC 2011. The genetic architecture of adaptation under migration–selection balance.
1164 Evolution 65: 1897-1911.

1165 Yin MB, Giessler S, Griebel J, Wolinska J 2014. Hybridizing *Daphnia* communities from ten neighbouring
1166 lakes: spatio-temporal dynamics, local processes, gene flow and invasiveness. Hybridizing *Daphnia*
1167 communities from ten neighbouring lakes: spatio-temporal dynamics, local processes, gene flow and
1168 invasiveness 14. doi: 10.1186/1471-2148-14-80

1169 Zehnder A, Gorham PR 1960. Factors influencing the growth of *Microcystis aeruginosa* Kütz. Emend.
1170 Elenkin. Can. J. Microbiol 6: 645-660.

1171 Zheng X*, et al.* 2012. A high-performance computing toolset for relatedness and principal component
1172 analysis of SNP data. Bioinformatics 28: 3326-3328.

1173